

Dihedral Razumov–Stroganov conjecture: a refined version



UNIVERSITÀ DEGLI STUDI
DI MILANO

Andrea Sportiello

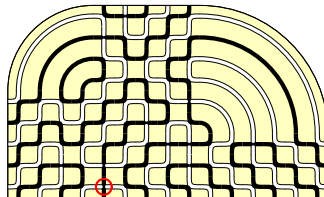
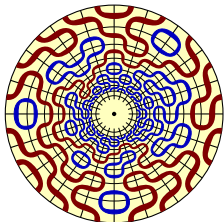
work in collaboration with L. Cantini

Journées de Combinatoire de Bordeaux 2012

LaBRI

Université de Bordeaux I

February 3rd 2012



Three Random Tiling Problems

O(1) Dense Loop Model

XXZ Quantum Spin Chain at $\Delta = -\frac{1}{2}$

Edge-percolation (Potts Model at $Q = 1$)

–

Fully-Packed Loops (FPL) in a square

Alternating Sign Matrices (ASM)

Six-Vertex Model at $\Delta = +\frac{1}{2}$ (Ice Model)

“Gog” triangles

–

TSSCPP (Plane Partitions)

Dimer coverings / Lozenge tilings

NILP (Non-intersecting Lattice Paths)

“Magog” triangles

Three Random Tiling Problems

► **O(1) Dense Loop Model**

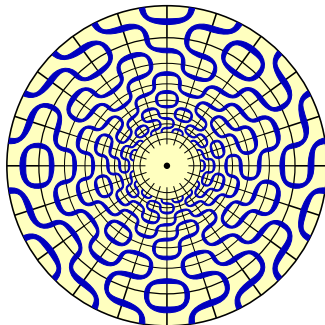
XXZ Quantum Spin Chain at $\Delta = -\frac{1}{2}$
Edge-percolation (Potts Model at $Q = 1$)

–

Fully-Packed Loops (FPL) in a square
Alternating Sign Matrices (ASM)
Six-Vortex Model at $\Delta = +\frac{1}{2}$ (Ice Model)
“Gog” triangles

–

TSSCPP (Plane Partitions)
Dimer coverings / Lozenge tilings
NILP (Non-intersecting Lattice Paths)
“Magog” triangles



Three Random Tiling Problems

O(1) Dense Loop Model

XXZ Quantum Spin Chain at $\Delta = -\frac{1}{2}$

Edge-percolation (Potts Model at $Q = 1$)

–

- ➔ **Fully-Packed Loops** (FPL) in a square
- Alternating Sign Matrices (ASM)
- Six-Vortex Model at $\Delta = +\frac{1}{2}$ (Ice Model)
- “Gog” triangles

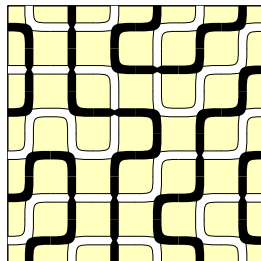
–

TSSCPP (Plane Partitions)

Dimer coverings / Lozenge tilings

NILP (Non-intersecting Lattice Paths)

“Magog” triangles



Three Random Tiling Problems

O(1) Dense Loop Model

XXZ Quantum Spin Chain at $\Delta = -\frac{1}{2}$

Edge-percolation (Potts Model at $Q = 1$)

–

Fully-Packed Loops (FPL) in a square

Alternating Sign Matrices (ASM)

Six-Vortex Model at $\Delta = +\frac{1}{2}$ (Ice Model)

“Gog” triangles

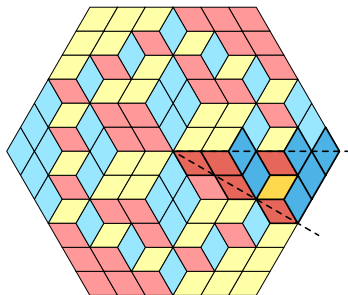
–

➔ **TSSCPP** (Plane Partitions)

Dimer coverings / Lozenge tilings

NILP (Non-intersecting Lattice Paths)

“Magog” triangles



Three Random Tiling Problems

O(1) Dense Loop Model

XXZ Quantum Spin Chain at $\Delta = -\frac{1}{2}$
Edge-percolation (Potts Model at $Q = 1$)

–

Fully-Packed Loops (FPL) in a square
Alternating Sign Matrices (ASM)

Six-Vortex Model at $\Delta = +\frac{1}{2}$ (Ice Model)

“Gog” triangles

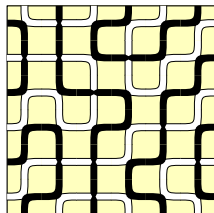
–

TSSCPP (Plane Partitions)

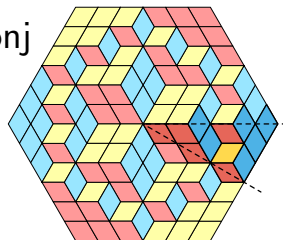
Dimer coverings / Lozenge tilings

NILP (Non-intersecting Lattice Paths)

“Magog” triangles



ASM-conj



Three Random Tiling Problems

O(1) Dense Loop Model

XXZ Quantum Spin Chain at $\Delta = -\frac{1}{2}$
Edge-percolation (Potts Model at $Q = 1$)

–

Fully-Packed Loops (FPL) in a square
Alternating Sign Matrices (ASM)

Six-Vortex Model at $\Delta = +\frac{1}{2}$ (Ice Model)

“Gog” triangles

–

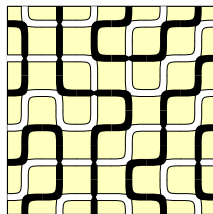
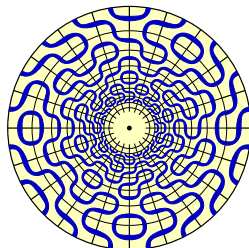
TSSCPP (Plane Partitions)

Dimer coverings / Lozenge tilings

NILP (Non-intersecting Lattice Paths)

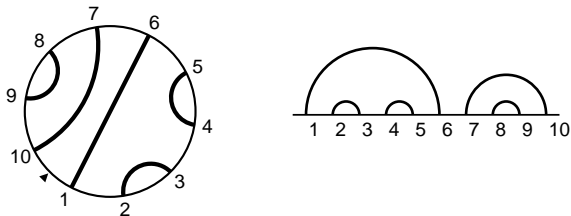
“Magog” triangles

•
•
•
RS
•
•



Link patterns

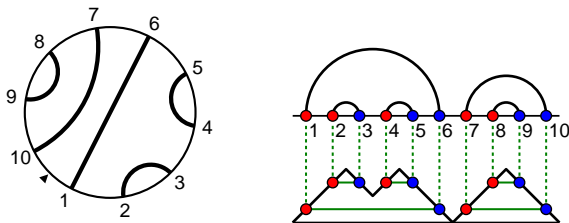
A **link pattern** $\pi \in \mathcal{LP}(2n)$ is a pairing of $\{1, 2, \dots, 2n\}$ having no pairs $(a, c), (b, d)$ such that $a < b < c < d$ (i.e., the drawing consists of n **non-crossing** arcs).



They are $C_n = \frac{1}{n+1} \binom{2n}{n}$ (the n -th *Catalan number*),

Link patterns

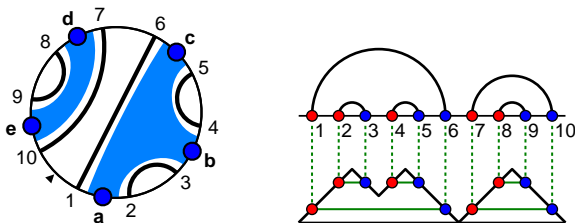
A **link pattern** $\pi \in \mathcal{LP}(2n)$ is a pairing of $\{1, 2, \dots, 2n\}$ having no pairs $(a, c), (b, d)$ such that $a < b < c < d$ (i.e., the drawing consists of n **non-crossing** arcs).



They are $C_n = \frac{1}{n+1} \binom{2n}{n}$ (the n -th *Catalan number*),
are in easy bijection with **Dyck Paths** of length $2n$

Link patterns

A **link pattern** $\pi \in \mathcal{LP}(2n)$ is a pairing of $\{1, 2, \dots, 2n\}$ having no pairs $(a, c), (b, d)$ such that $a < b < c < d$ (i.e., the drawing consists of n **non-crossing** arcs).

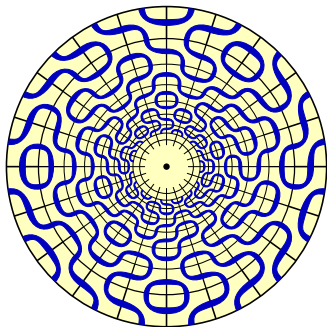


They are $C_n = \frac{1}{n+1} \binom{2n}{n}$ (the n -th *Catalan number*), are in easy bijection with **Dyck Paths** of length $2n$ and with **non-crossing partitions** of n elements.

...and many other things...

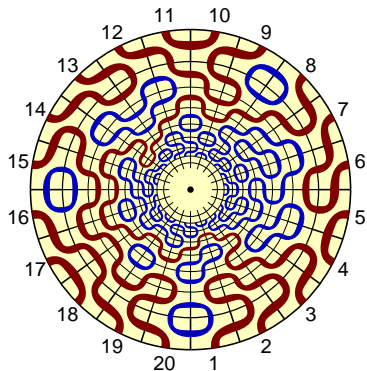
Link patterns in the Dense Loop Model

To a **dense-loop** configuration on a semi-infinite cylinder, a **link pattern** π is naturally associated, as the connectivity pattern for the points on the boundary.



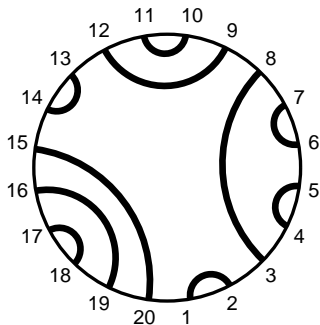
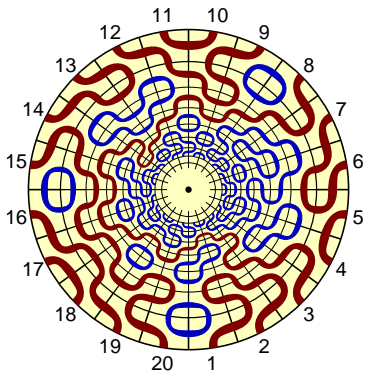
Link patterns in the Dense Loop Model

To a **dense-loop** configuration on a semi-infinite cylinder, a **link pattern** π is naturally associated, as the connectivity pattern for the points on the boundary.



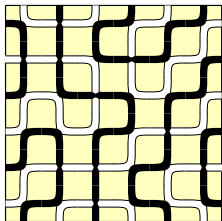
Link patterns in the Dense Loop Model

To a **dense-loop** configuration on a semi-infinite cylinder, a **link pattern** π is naturally associated, as the connectivity pattern for the points on the boundary.



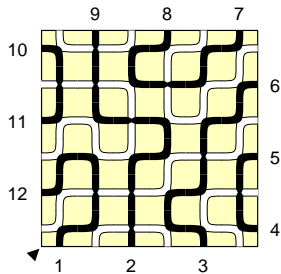
Link patterns in Fully-Packed Loops

To a Fully-Packed Loop configuration, a link pattern π is naturally associated, from connectivities among the black terminations on the boundary.



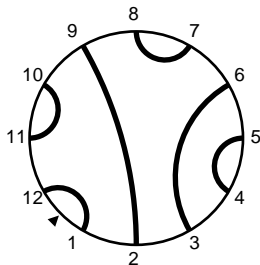
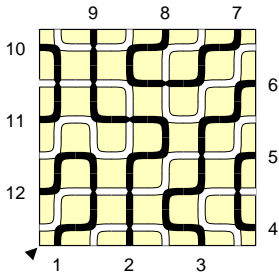
Link patterns in Fully-Packed Loops

To a Fully-Packed Loop configuration, a link pattern π is naturally associated, from connectivities among the black terminations on the boundary.

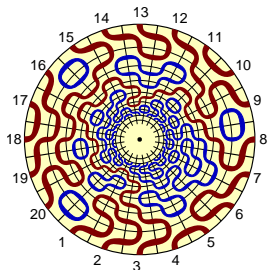


Link patterns in Fully-Packed Loops

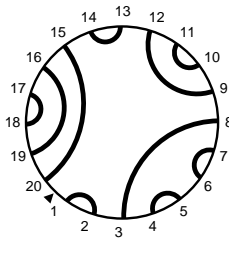
To a Fully-Packed Loop configuration, a link pattern π is naturally associated, from connectivities among the black terminations on the boundary.



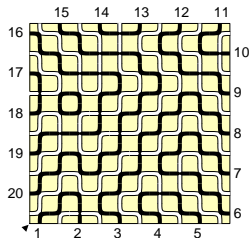
The Razumov–Stroganov correspondence



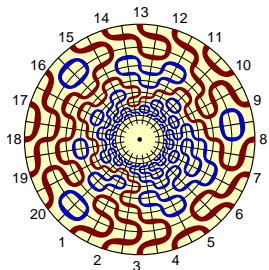
$\tilde{\Psi}_n(\pi)$: probability of π
in the $O(1)$ Dense Loop Model
in the $\{1, \dots, 2n\} \times \mathbb{N}$ cylinder



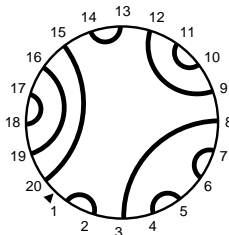
$\Psi_n(\pi)$: probability of π
for FPL with uniform measure
in the $n \times n$ square



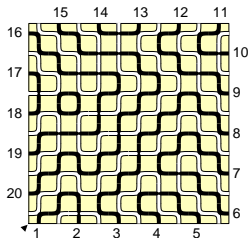
The Razumov–Stroganov correspondence



$\tilde{\Psi}_n(\pi)$: probability of π
in the $O(1)$ Dense Loop Model
in the $\{1, \dots, 2n\} \times \mathbb{N}$ cylinder



$\Psi_n(\pi)$: probability of π
for FPL with uniform measure
in the $n \times n$ square



Razumov–Stroganov correspondence

(conjecture: Razumov Stroganov, 2001; proof: AS Cantini, 2010)

$$\tilde{\Psi}_n(\pi) = \Psi_n(\pi)$$

Dihedral symmetry of FPL

A corollary of the Razumov–Stroganov correspondence. . .

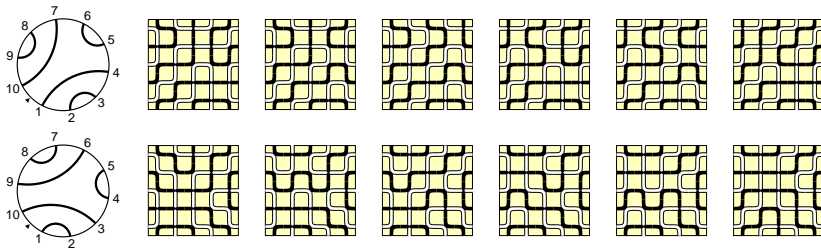
(. . . that was known *before* the Razumov–Stroganov conjecture)

call R the operator that rotates a link pattern by one position

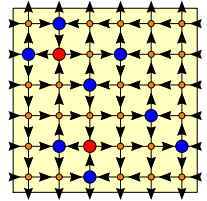
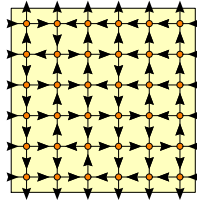
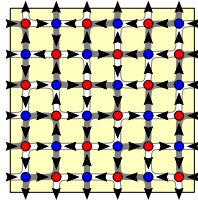
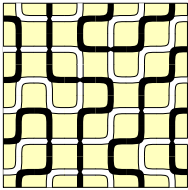
Dihedral symmetry of FPL

(proof: Wieland, 2000)

$$\Psi_n(\pi) = \Psi_n(R\pi)$$

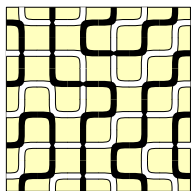


Fully-Packed Loops \Rightarrow 6VM \Rightarrow Alternating Sign Matrices

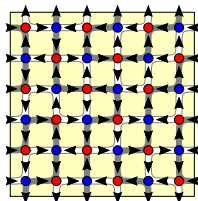


FPL
config

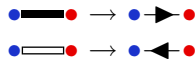
Fully-Packed Loops \Rightarrow 6VM \Rightarrow Alternating Sign Matrices



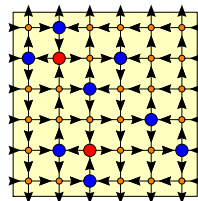
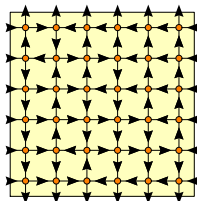
FPL
config



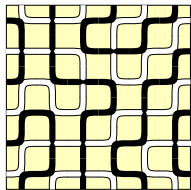
• or • according
to parity;



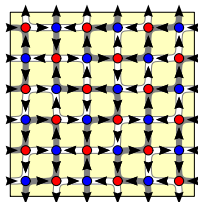
Forget parity;



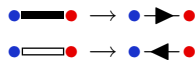
Fully-Packed Loops \Rightarrow 6VM \Rightarrow Alternating Sign Matrices



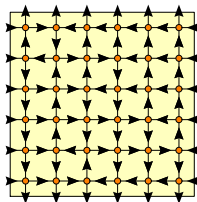
FPL
config



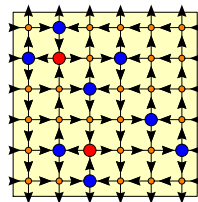
● or ● according
to parity;



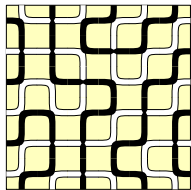
Forget parity;



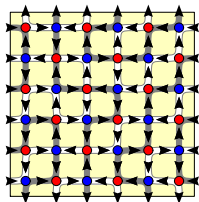
6-vertex
config
(DWBC)



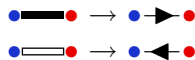
Fully-Packed Loops \Rightarrow 6VM \Rightarrow Alternating Sign Matrices



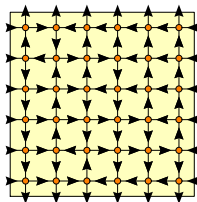
FPL
config



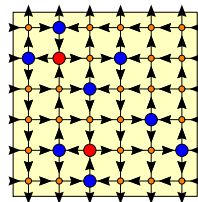
● or ● according
to parity;



Forget parity;

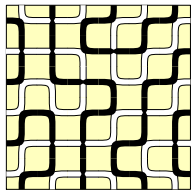


6-vertex
config
(DWBC)

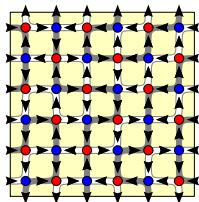


Arrow directions
along rows/cols
get flipped at ●, ●

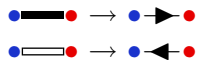
Fully-Packed Loops \Rightarrow 6VM \Rightarrow Alternating Sign Matrices



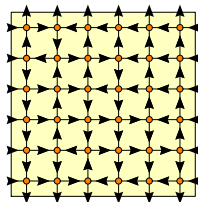
FPL
config



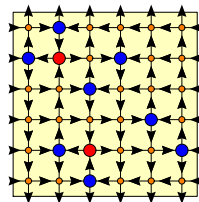
• or • according to parity;
to parity;



Forget parity;



6-vertex
config
(DWBC)



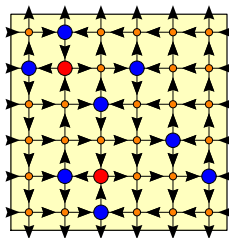
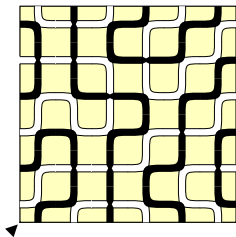
Arrow directions
along rows/cols
get flipped at •, •

ASM config

0	+1	0	0	0	0
+1	-1	0	+1	0	0
0	0	+1	0	0	0
0	0	0	0	+1	0
0	+1	-1	0	0	+1
0	0	+1	0	0	0

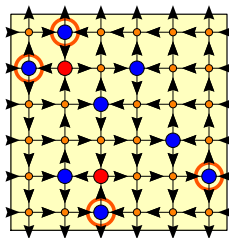
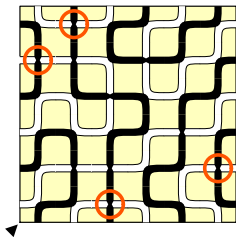
Refinement position in Fully-Packed Loops

Fully-Packed Loops have a **unique** straight tile on any external line
Alternating Sign Matrices have a **unique** +1 on any external line



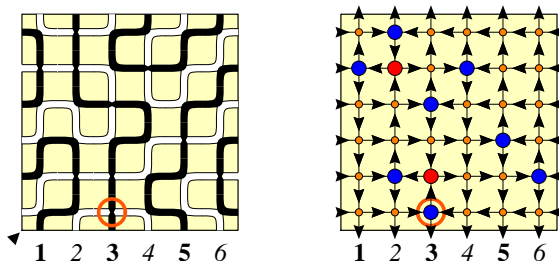
Refinement position in Fully-Packed Loops

Fully-Packed Loops have a **unique** straight tile on any external line
Alternating Sign Matrices have a **unique** +1 on any external line



Refinement position in Fully-Packed Loops

Fully-Packed Loops have a **unique** straight tile on any external line
Alternating Sign Matrices have a **unique** +1 on any external line



Concentrate on the bottom row, and call **refinement position** the corresponding column index.

The Temperley-Lieb(1) monoid

Consider the **graphical action** over **link patterns** $\pi \in \mathcal{LP}(2n)$
(throw away detached cycles)

$$R : \begin{array}{c} \text{77777777} \\ 1 \ 2 \ 3 \ \dots \quad 2n \end{array} \quad e_j : \begin{array}{c} | \ | \ | \ \dots \ | \ \cup \ | \ \dots \ | \\ 1 \ 2 \ 3 \ \dots \quad j \ j+1 \ \dots 2n \end{array}$$

The maps $\{e_j\}_{1 \leq j \leq 2n}$ and $R^{\pm 1}$ generate a **semigroup**

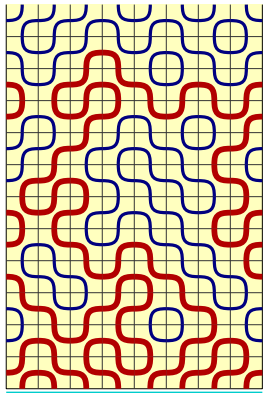
Example:

$$e_1(\pi) : \begin{array}{c} \text{Diagram with arcs (1,2), (2,3), (3,4), (4,5), (5,6), (7,8), (8,9), (9,10)} \\ 1 \ 2 \ 3 \ 4 \ 5 \ 6 \ 7 \ 8 \ 9 \ 10 \end{array} = \begin{array}{c} \text{Diagram with arcs (1,2), (3,4), (5,6), (7,8), (9,10)} \\ 1 \ 2 \ 3 \ 4 \ 5 \ 6 \ 7 \ 8 \ 9 \ 10 \end{array}$$

$$e_2(\pi) : \begin{array}{c} \text{Diagram with arcs (1,2), (2,3), (3,4), (4,5), (5,6), (7,8), (8,9), (9,10)} \\ 1 \ 2 \ 3 \ 4 \ 5 \ 6 \ 7 \ 8 \ 9 \ 10 \end{array} = \begin{array}{c} \text{Diagram with arcs (1,2), (3,4), (5,6), (7,8), (9,10)} \\ 1 \ 2 \ 3 \ 4 \ 5 \ 6 \ 7 \ 8 \ 9 \ 10 \end{array}$$

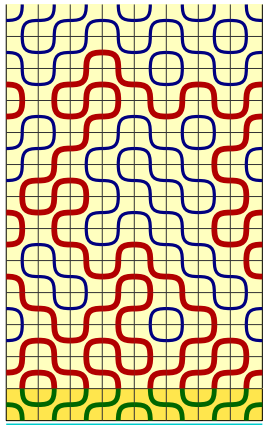
Consider the **linear space** $\mathbb{C}^{\mathcal{LP}(2n)}$, linear span of **basis vectors** $|\pi\rangle$.
 Operators e_j and $R^{\pm 1}$ are **linear operators** over $\mathbb{C}^{\mathcal{LP}(2n)}$

$O(1)$ dense loop model: the Markov Chain over $\mathcal{LP}(2n)$



A config with $t - 1$ layers.

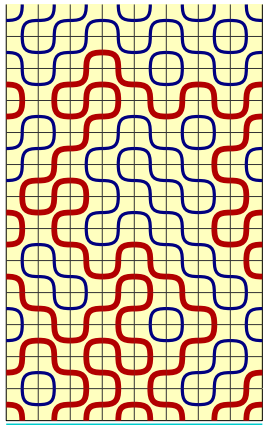
$O(1)$ dense loop model: the Markov Chain over $\mathcal{LP}(2n)$



A config with $t - 1$ layers.

Add a new layer, of i.i.d. tiles, with prob. p (say, $p = 1/2$)...

$O(1)$ dense loop model: the Markov Chain over $\mathcal{LP}(2n)$



A config with $t - 1$ layers.

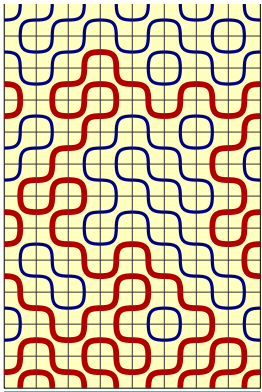
Add a new layer, of i.i.d. tiles, with prob. p (say, $p = 1/2$)...

Some loops get detached from the boundary. You have a config with t layers, and a new link pattern.

$$\text{Rates } T_{p=1/2}(\pi, \pi')$$

$O(1)$ dense loop model: the Markov Chain over $\mathcal{LP}(2n)$

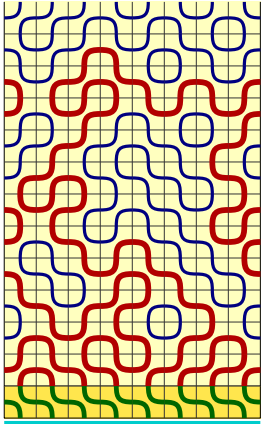
Now repeat the game...



$O(1)$ dense loop model: the Markov Chain over $\mathcal{LP}(2n)$

Now repeat the game...

...but add i.i.d. tiles, with prob.
 $p \rightarrow 0$...

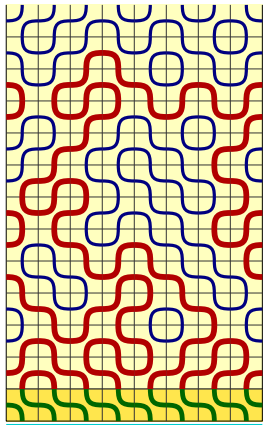


$O(1)$ dense loop model: the Markov Chain over $\mathcal{LP}(2n)$

Now repeat the game...

...but add i.i.d. tiles, with prob.
 $p \rightarrow 0$...

For most of the layers you just rotate...



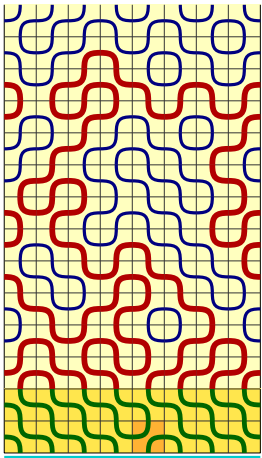
$O(1)$ dense loop model: the Markov Chain over $\mathcal{LP}(2n)$

Now repeat the game...

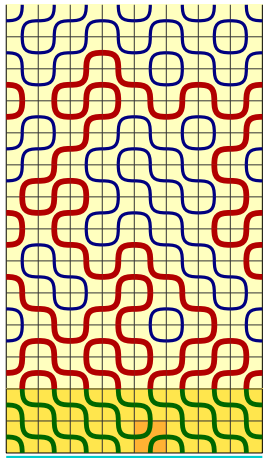
...but add i.i.d. tiles, with prob.
 $p \rightarrow 0$...

For most of the layers you just rotate... From time to time, you have a single non-trivial tile.

$$\text{Rates } T_{p \rightarrow 0}(\pi, \pi')$$



$O(1)$ dense loop model: the Markov Chain over $\mathcal{LP}(2n)$



Now repeat the game...

...but add i.i.d. tiles, with prob.
 $p \rightarrow 0$...

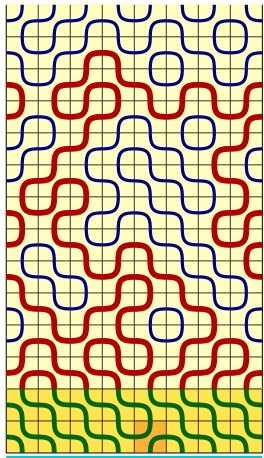
For most of the layers you just rotate... From time to time, you have a single non-trivial tile.

$$\text{Rates } T_{p \rightarrow 0}(\pi, \pi')$$

Non-trivial layers look like
operators $R e_j$

$$T_p = R(I + p \sum_j (e_j - 1) + \mathcal{O}(p^2))$$

$O(1)$ dense loop model: the Markov Chain over $\mathcal{LP}(2n)$



Now repeat the game...

...but add i.i.d. tiles, with prob.
 $p \rightarrow 0$...

For most of the layers you just rotate... From time to time, you have a single non-trivial tile.

$$\text{Rates } T_{p \rightarrow 0}(\pi, \pi')$$

Non-trivial layers look like
operators $R e_j$

$$T_p = R(l + p \sum_j (e_j - 1) + \mathcal{O}(p^2))$$

Hamiltonian H

Integrability: commutation of Transfer Matrices

Call $T_p(\pi, \pi')$ the matrix of transition rates, acting on $\mathbb{C}^{\mathcal{L}P(2n)}$ for tiling one layer, with probability p .

Trivial: $\tilde{\Psi}_p(\pi)$, the steady state, is the **unique** eigenstate of $T_p(\pi, \pi')$ with all positive entries

The Yang–Baxter relation implies: $[T_p, T_{p'}] = 0$

Consequence: $\tilde{\Psi}_p(\pi) \equiv \tilde{\Psi}_{p'}(\pi)$ and we can get $\tilde{\Psi}(\pi) := \tilde{\Psi}_{1/2}(\pi)$ from the study of the easier $T_{p \rightarrow 0}(\pi, \pi')$

Call $H_n = \sum_{i=1}^{2n} (e_i - 1)$ and $|\tilde{\Psi}_n\rangle = \sum_{\pi} \tilde{\Psi}(\pi) |\pi\rangle$

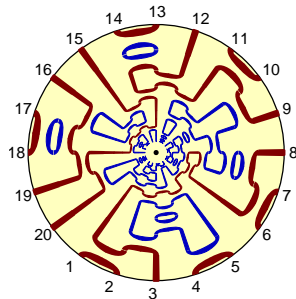
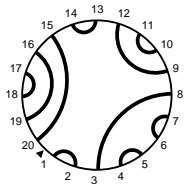
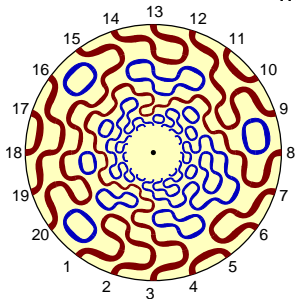
As $R^{-1}T_p = I + pH + \mathcal{O}(p^2)$ we have

$$H_n |\tilde{\Psi}_n\rangle = 0$$

linear-algebra characterization of $\tilde{\Psi}(\pi)$

Integrability: commutation of Transfer Matrices

...said with a picture...



$$|\tilde{\Psi}_n\rangle := \sum_{\pi \in \mathcal{LP}(2n)} \tilde{\Psi}_n(\pi) |\pi\rangle$$

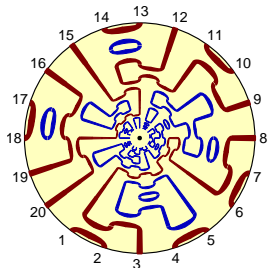
$$(T_n - 1)|\tilde{\Psi}_n\rangle = 0$$

$$|\tilde{\Psi}_n\rangle := \sum_{\pi \in \mathcal{LP}(2n)} \tilde{\Psi}_n(\pi) |\pi\rangle$$

$$H_n|\tilde{\Psi}_n\rangle = 0$$

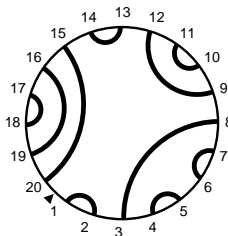
the two linear equations for $|\tilde{\Psi}_n\rangle$ are equivalent!

The Razumov–Stroganov correspondence: reloaded



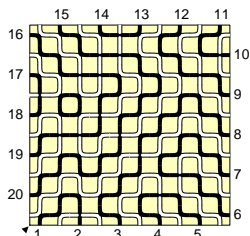
$$|\tilde{\Psi}_n\rangle := \sum_{\pi \in \mathcal{LP}(2n)} \tilde{\Psi}_n(\pi) |\pi\rangle$$

$$H_n |\tilde{\Psi}_n\rangle = 0$$

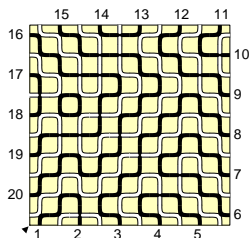
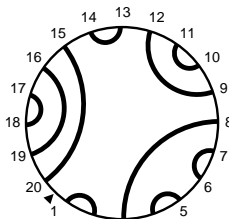
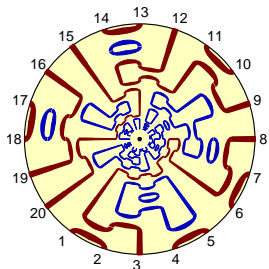


$$|\Psi_n\rangle = \sum_{\phi \in \mathcal{Fpl}(n)} |\pi(\phi)\rangle$$

$$\mathcal{Fpl}(n) = \{ \text{FPL in } n \times n \text{ square} \}$$



The Razumov–Stroganov correspondence: reloaded



$$|\tilde{\Psi}_n\rangle := \sum_{\pi \in \mathcal{LP}(2n)} \tilde{\Psi}_n(\pi) |\pi\rangle$$

$$H_n |\tilde{\Psi}_n\rangle = 0$$

$$|\Psi_n\rangle = \sum_{\phi \in \mathcal{Fpl}(n)} |\pi(\phi)\rangle$$

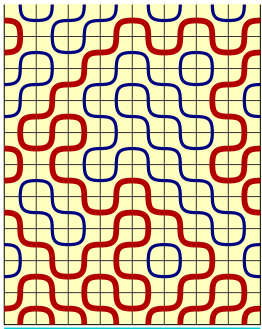
$$\mathcal{Fpl}(n) = \{ \text{FPL in } n \times n \text{ square} \}$$

Razumov–Stroganov correspondence

(conjecture: Razumov Stroganov, 2001; proof: AS Cantini, 2010)

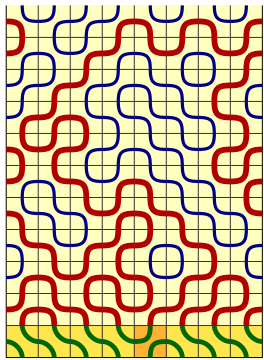
$$H_n |\Psi_n\rangle = 0$$

$O(1)$ dense loop model: the Scattering Matrices



Repeat the game once more...

$O(1)$ dense loop model: the Scattering Matrices



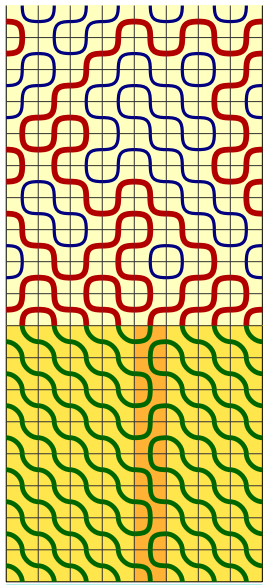
Repeat the game once more...

...but this time keep all tiles frozen, except for the one in column $i + 1$

$$RX_i(t) = R(t + (1 - t)e_i)$$

...ok, these operators by themselves are not specially nice, nonetheless...

$O(1)$ dense loop model: the Scattering Matrices



Repeat the game once more...

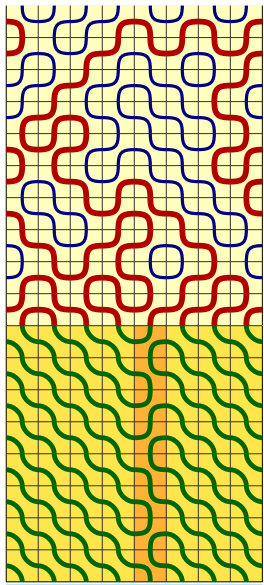
...but this time keep all tiles frozen, except for the one in column $i + 1$

$$RX_i(t) = R(t + (1 - t)e_i)$$

...ok, these operators by themselves are not specially nice, nonetheless...

...call $S_i(t) = (RX_i(t))^N$
the **Scattering Matrix** on column i .

$O(1)$ dense loop model: the Scattering Matrices



Repeat the game once more...

...but this time keep all tiles frozen, except for the one in column $i + 1$

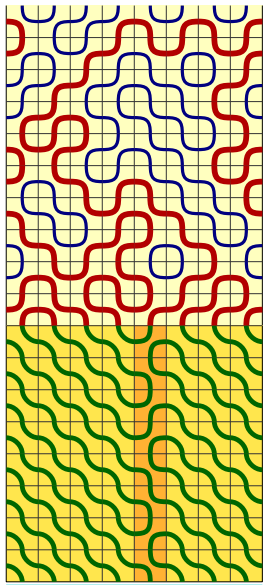
$$RX_i(t) = R(t + (1 - t)e_i)$$

...ok, these operators by themselves are not specially nice, nonetheless...

...call $S_i(t) = (RX_i(t))^N$
the **Scattering Matrix** on column i .

$[S_i(t), S_i(t')]$ is ugly

$O(1)$ dense loop model: the Scattering Matrices



Repeat the game once more...

...but this time keep all tiles frozen, except for the one in column $i + 1$

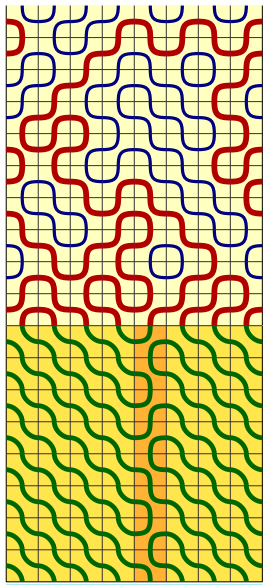
$$RX_i(t) = R(t + (1 - t)e_i)$$

...ok, these operators by themselves are not specially nice, nonetheless...

...call $S_i(t) = (RX_i(t))^N$
the **Scattering Matrix** on column i .

$[S_i(t), S_j(t)]$ is ugly

$O(1)$ dense loop model: the Scattering Matrices



Repeat the game once more...

...but this time keep all tiles frozen, except for the one in column $i + 1$

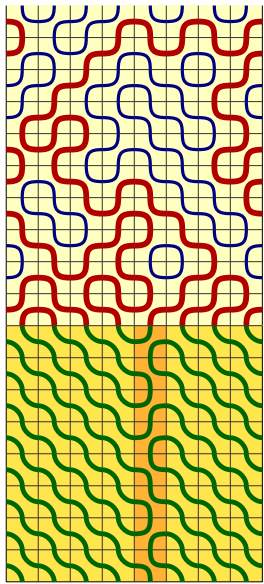
$$RX_i(t) = R(t + (1 - t)e_i)$$

...ok, these operators by themselves are not specially nice, nonetheless...

...call $S_i(t) = (RX_i(t))^N$
the **Scattering Matrix** on column i .

$[S_i(t), T(\rho)]$ is ugly

$O(1)$ dense loop model: the Scattering Matrices



Repeat the game once more...

...but this time keep all tiles frozen, except for the one in column $i + 1$

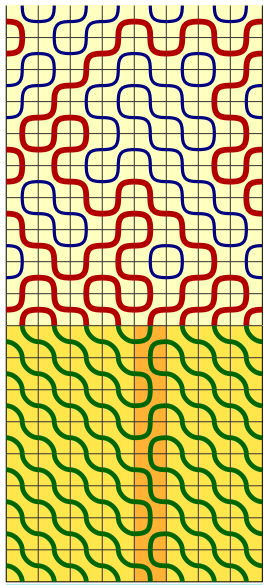
$$RX_i(t) = R(t + (1 - t)e_i)$$

...ok, these operators by themselves are not specially nice, nonetheless...

...call $S_i(t) = (RX_i(t))^N$
the **Scattering Matrix** on column i .

$[S_i(t), H]$ is ugly...

$O(1)$ dense loop model: the Scattering Matrices



Repeat the game once more...

...but this time keep all tiles frozen, except for the one in column $i + 1$

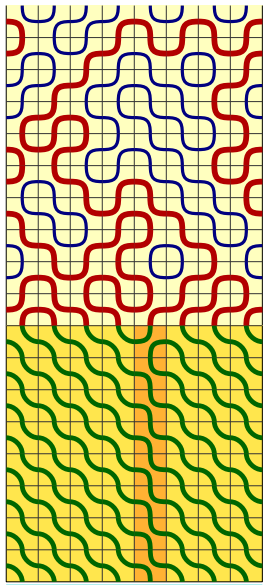
$$RX_i(t) = R(t + (1 - t)e_i)$$

...ok, these operators by themselves are not specially nice, nonetheless...

...call $S_i(t) = (RX_i(t))^N$
the **Scattering Matrix** on column i .

...but $S_i(1 - t) = \mathbf{1} + t H + \mathcal{O}(t^2)$

$O(1)$ dense loop model: the Scattering Matrices



Repeat the game once more...

...but this time keep all tiles frozen, except for the one in column $i + 1$

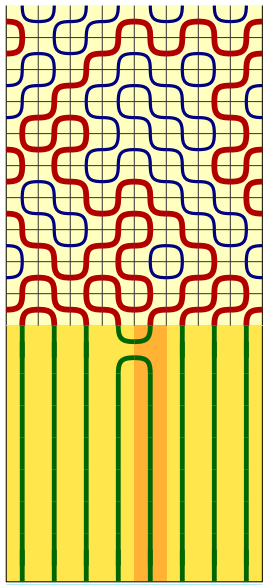
$$RX_i(t) = R(t + (1 - t)e_i)$$

...ok, these operators by themselves are not specially nice, nonetheless...

...call $S_i(t) = (RX_i(t))^N$
the **Scattering Matrix** on column i .

...but $S_i(1 - t) = \mathbf{1} + t H + \mathcal{O}(t^2)$

$O(1)$ dense loop model: the Scattering Matrices



Repeat the game once more...

...but this time keep all tiles frozen, except for the one in column $i + 1$

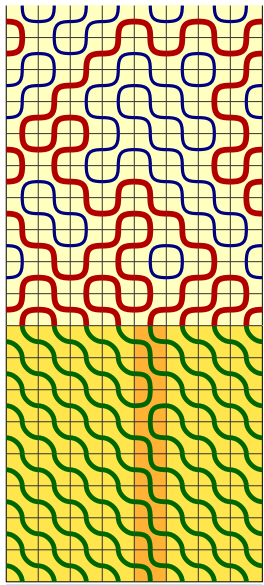
$$RX_i(t) = R(t + (1 - t)e_i)$$

...ok, these operators by themselves are not specially nice, nonetheless...

...call $S_i(t) = (RX_i(t))^N$
the **Scattering Matrix** on column i .

...but $S_i(1 - t) = \mathbf{1} + t H + \mathcal{O}(t^2)$

$O(1)$ dense loop model: the Scattering Matrices



Repeat the game once more...

...but this time keep all tiles frozen, except for the one in column $i + 1$

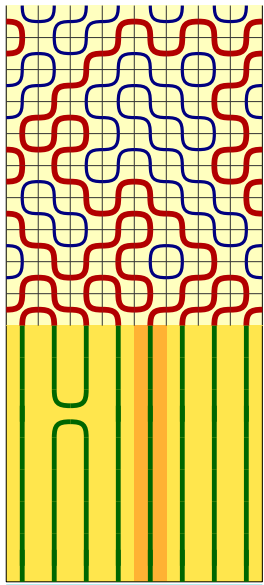
$$RX_i(t) = R(t + (1 - t)e_i)$$

...ok, these operators by themselves are not specially nice, nonetheless...

...call $S_i(t) = (RX_i(t))^N$
the **Scattering Matrix** on column i .

...but $S_i(1 - t) = \mathbf{1} + t H + \mathcal{O}(t^2)$

$O(1)$ dense loop model: the Scattering Matrices



Repeat the game once more...

...but this time keep all tiles frozen, except for the one in column $i + 1$

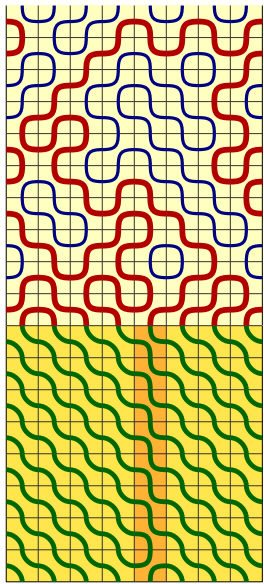
$$RX_i(t) = R(t + (1 - t)e_i)$$

...ok, these operators by themselves are not specially nice, nonetheless...

...call $S_i(t) = (RX_i(t))^N$
the **Scattering Matrix** on column i .

...but $S_i(1 - t) = \mathbf{1} + t H + \mathcal{O}(t^2)$

$O(1)$ dense loop model: the Scattering Matrices



Repeat the game once more...

...but this time keep all tiles frozen, except for the one in column $i + 1$

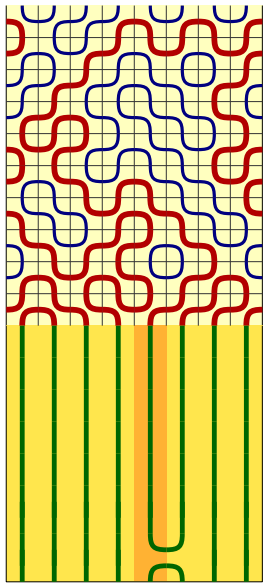
$$RX_i(t) = R(t + (1 - t)e_i)$$

...ok, these operators by themselves are not specially nice, nonetheless...

...call $S_i(t) = (RX_i(t))^N$
the **Scattering Matrix** on column i .

...but $S_i(1 - t) = \mathbf{1} + t H + \mathcal{O}(t^2)$

$O(1)$ dense loop model: the Scattering Matrices



Repeat the game once more...

...but this time keep all tiles frozen, except for the one in column $i + 1$

$$RX_i(t) = R(t + (1 - t)e_i)$$

...ok, these operators by themselves are not specially nice, nonetheless...

...call $S_i(t) = (RX_i(t))^N$
the **Scattering Matrix** on column i .

...but $S_i(1 - t) = \mathbf{1} + t H + \mathcal{O}(t^2)$

Dihedral covariance of the ground states

We had $|\tilde{\Psi}_n\rangle = \sum_{\pi} \tilde{\Psi}(\pi)|\pi\rangle$, satisfying $H_n|\tilde{\Psi}_n\rangle = 0$

The operators $RX_i(t)$, and the scattering matrices $S_i(t)$,
induce the deformation

$$|\tilde{\Psi}_n^{(i)}(t)\rangle = \sum_{\pi} \tilde{\Psi}^{(i)}(t; \pi)|\pi\rangle, \text{ satisfying } (RX_i(t) - 1)|\tilde{\Psi}_n^{(i)}(t)\rangle = 0.$$

Because of a **dihedral covariance** of these equations,
(and unicity of the Frobenius vector)
it suffices to study $RX_1(t)$ and $|\tilde{\Psi}_n^{(1)}(t)\rangle$

Example:

$$0 = (X_i(t) - R^{-1})|\tilde{\Psi}_n^{(i)}(t)\rangle = R(X_{i+1}(t) - R^{-1})R^{-1}|\tilde{\Psi}_n^{(i)}(t)\rangle$$

implying $|\tilde{\Psi}_n^{(i+1)}(t)\rangle \propto R^{-1}|\tilde{\Psi}_n^{(i)}(t)\rangle$

Call $\text{Sym} = N^{-1} \sum_{i=0}^{N-1} R^i$, the operator that projects on the rotationally-invariant subspace of $\mathbb{C}^{\text{LP}(N)}$.

Dihedral covariance of the ground states

We had $|\tilde{\Psi}_n\rangle = \sum_{\pi} \tilde{\Psi}(\pi)|\pi\rangle$, satisfying $H_n|\tilde{\Psi}_n\rangle = 0$

The operators $RX_i(t)$, and the scattering matrices $S_i(t)$,
induce the deformation

$$|\tilde{\Psi}_n^{(i)}(t)\rangle = \sum_{\pi} \tilde{\Psi}^{(i)}(t; \pi)|\pi\rangle, \text{ satisfying } (RX_i(t) - 1)|\tilde{\Psi}_n^{(i)}(t)\rangle = 0.$$

Because of a **dihedral covariance** of these equations,
(and unicity of the Frobenius vector)
it suffices to study $RX_1(t)$ and $|\tilde{\Psi}_n^{(1)}(t)\rangle$

Example:

$$0 = (X_i(t) - R^{-1})|\tilde{\Psi}_n^{(i)}(t)\rangle = R(X_{i+1}(t) - R^{-1})R^{-1}|\tilde{\Psi}_n^{(i)}(t)\rangle$$

implying $|\tilde{\Psi}_n^{(i+1)}(t)\rangle \propto R^{-1}|\tilde{\Psi}_n^{(i)}(t)\rangle$

Call $\text{Sym} = N^{-1} \sum_{i=0}^{N-1} R^i$, the operator that **projects** on the
rotationally-invariant subspace of $\mathbb{C}^{\text{LP}(N)}$.

Dihedral covariance of the ground states

We had $|\tilde{\Psi}_n\rangle = \sum_{\pi} \tilde{\Psi}(\pi)|\pi\rangle$, satisfying $H_n|\tilde{\Psi}_n\rangle = 0$

The operators $RX_i(t)$, and the scattering matrices $S_i(t)$,
induce the deformation

$$|\tilde{\Psi}_n^{(i)}(t)\rangle = \sum_{\pi} \tilde{\Psi}^{(i)}(t; \pi)|\pi\rangle, \text{ satisfying } (RX_i(t) - 1)|\tilde{\Psi}_n^{(i)}(t)\rangle = 0.$$

Because of a **dihedral covariance** of these equations,
(and unicity of the Frobenius vector)
it suffices to study $RX_1(t)$ and $|\tilde{\Psi}_n^{(1)}(t)\rangle$

Example:

$$0 = (X_i(t) - R^{-1})|\tilde{\Psi}_n^{(i)}(t)\rangle = R(X_{i+1}(t) - R^{-1})R^{-1}|\tilde{\Psi}_n^{(i)}(t)\rangle$$

implying $|\tilde{\Psi}_n^{(i+1)}(t)\rangle \propto R^{-1}|\tilde{\Psi}_n^{(i)}(t)\rangle$

Call $\text{Sym} = N^{-1} \sum_{i=0}^{N-1} R^i$, the operator that **projects** on the
rotationally-invariant subspace of $\mathbb{C}^{\mathcal{L}P(N)}$.

Dihedral covariance of the ground states

We had $|\tilde{\Psi}_n\rangle = \sum_{\pi} \tilde{\Psi}(\pi)|\pi\rangle$, satisfying $H_n|\tilde{\Psi}_n\rangle = 0$

The operators $RX_i(t)$, and the scattering matrices $S_i(t)$,
induce the deformation

$$|\tilde{\Psi}_n^{(i)}(t)\rangle = \sum_{\pi} \tilde{\Psi}^{(i)}(t; \pi)|\pi\rangle, \text{ satisfying } (RX_i(t) - 1)|\tilde{\Psi}_n^{(i)}(t)\rangle = 0.$$

Because of a **dihedral covariance** of these equations,
(and unicity of the Frobenius vector)
it suffices to study $RX_1(t)$ and $|\tilde{\Psi}_n^{(1)}(t)\rangle$

Example:

$$0 = (X_i(t) - R^{-1})|\tilde{\Psi}_n^{(i)}(t)\rangle = R(X_{i+1}(t) - R^{-1})R^{-1}|\tilde{\Psi}_n^{(i)}(t)\rangle$$

implying $|\tilde{\Psi}_n^{(i+1)}(t)\rangle \propto R^{-1}|\tilde{\Psi}_n^{(i)}(t)\rangle$

Call $\text{Sym} = N^{-1} \sum_{i=0}^{N-1} R^i$, the operator that **projects** on the
rotationally-invariant subspace of $\mathbb{C}^{\mathcal{L}\mathcal{P}(N)}$.

Dihedral covariance of the ground states

We had $|\tilde{\Psi}_n\rangle = \sum_{\pi} \tilde{\Psi}(\pi)|\pi\rangle$, satisfying $H_n|\tilde{\Psi}_n\rangle = 0$

The operators $RX_i(t)$, and the scattering matrices $S_i(t)$,
induce the deformation

$$|\tilde{\Psi}_n^{(i)}(t)\rangle = \sum_{\pi} \tilde{\Psi}^{(i)}(t; \pi)|\pi\rangle, \text{ satisfying } (RX_i(t) - 1)|\tilde{\Psi}_n^{(i)}(t)\rangle = 0.$$

Because of a **dihedral covariance** of these equations,
(and unicity of the Frobenius vector)
it suffices to study $RX_1(t)$ and $|\tilde{\Psi}_n^{(1)}(t)\rangle$

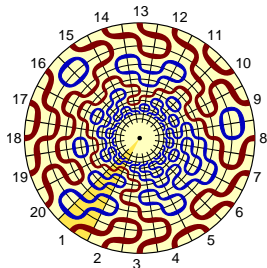
Example:

$$0 = (X_i(t) - R^{-1})|\tilde{\Psi}_n^{(i)}(t)\rangle = R(X_{i+1}(t) - R^{-1})R^{-1}|\tilde{\Psi}_n^{(i)}(t)\rangle$$

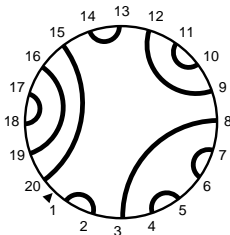
implying $|\tilde{\Psi}_n^{(i+1)}(t)\rangle \propto R^{-1}|\tilde{\Psi}_n^{(i)}(t)\rangle$

Call $\text{Sym} = N^{-1} \sum_{i=0}^{N-1} R^i$, the operator that **projects** on the rotationally-invariant subspace of $\mathbb{C}^{\mathcal{L}\mathcal{P}(N)}$.

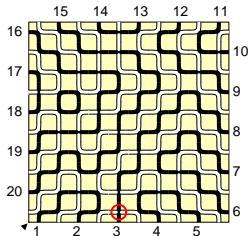
The refined Razumov–Stroganov correspondence



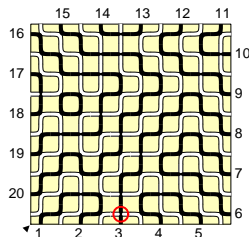
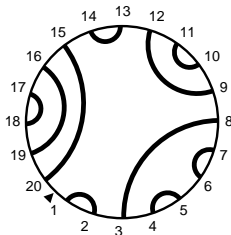
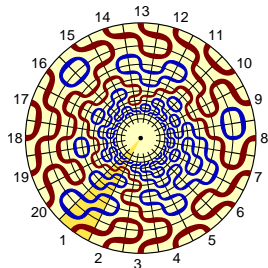
$\tilde{\Psi}_n(t; \pi)$: probability of π
in the $O(1)$ Dense Loop Model
with dynamics given by $RX_1(t)$



$\Psi_n(t; \pi)$: count FPL's ϕ
having link pattern π
give $t^{h(\phi)-1}$ weight



The refined Razumov–Stroganov correspondence



$\tilde{\Psi}_n(t; \pi)$: probability of π
in the $O(1)$ Dense Loop Model
with dynamics given by $RX_1(t)$

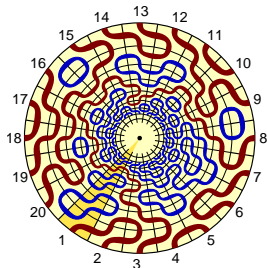
$\Psi_n(t; \pi)$: count FPL's ϕ
having link pattern π
give $t^{h(\phi)-1}$ weight

Refined Razumov–Stroganov correspondence

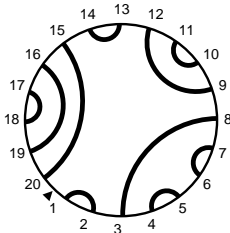
(conjecture: Di Francesco, 2004; proof: AS Cantini, 2012)

$$\tilde{\Psi}_n(t; \pi) \neq \Psi_n(t; \pi)$$

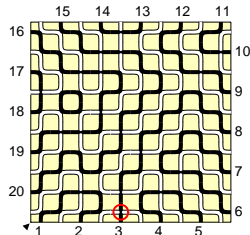
The refined Razumov–Stroganov correspondence



$\tilde{\Psi}_n(t; \pi)$: probability of π
in the $O(1)$ Dense Loop Model
with dynamics given by $RX_1(t)$



$\Psi_n(t; \pi)$: count FPL's ϕ
having link pattern π
give $t^{h(\phi)-1}$ weight

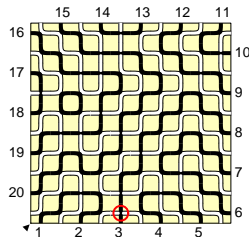
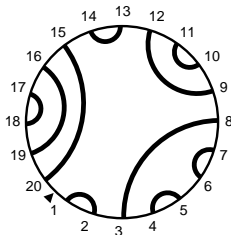
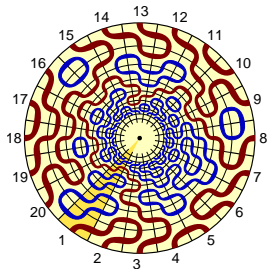


Refined Razumov–Stroganov correspondence

(conjecture: Di Francesco, 2004; proof: AS Cantini, 2012)

$$|\tilde{\Psi}_n(t)\rangle \neq |\Psi_n(t)\rangle$$

The refined Razumov–Stroganov correspondence



$\tilde{\Psi}_n(t; \pi)$: probability of π
in the $O(1)$ Dense Loop Model
with dynamics given by $RX_1(t)$

$\Psi_n(t; \pi)$: count FPL's ϕ
having link pattern π
give $t^{h(\phi)-1}$ weight

Refined Razumov–Stroganov correspondence

(conjecture: Di Francesco, 2004; proof: AS Cantini, 2012)

$$\text{Sym } |\tilde{\Psi}_n(t)\rangle = \text{Sym } |\Psi_n(t)\rangle$$

A quest for a new strategy

The strategy in the 2010 RS proof, by L. Cantini and me, was

- Realize that $H|\tilde{\Psi}\rangle = 0$ fixes $|\tilde{\Psi}\rangle$ univocally;
- Prove combinatorially that also $|\Psi\rangle$ satisfies $H|\Psi\rangle = 0$...

...But the $|\tilde{\Psi}^{(i)}\rangle$'s **differ** (they are only **dihedrally covariant**),
and satisfy **different** linear equations (with $RX_i(t)$)...

...and $\text{Sym } |\tilde{\Psi}^{(i)}\rangle$ does **not** satisfy any simple
linear equation that fixes it univocally!

Best possible hope:

- Find a **new way** $\pi'(\phi)$ of associating link patterns to FPL;
- Find&prove $|\tilde{\Psi}(t)\rangle = |\Psi'(t)\rangle$ **with no need of symmetrization**;
 - Prove **combinatorially** that $\text{Sym } |\Psi'(t)\rangle = \text{Sym } |\Psi(t)\rangle$

Bonus: The new enumeration is interesting by itself

A quest for a new strategy

The strategy in the 2010 RS proof, by L. Cantini and me, was

- Realize that $H|\tilde{\Psi}\rangle = 0$ fixes $|\tilde{\Psi}\rangle$ univocally;
- Prove combinatorially that also $|\Psi\rangle$ satisfies $H|\Psi\rangle = 0$...

...But the $|\tilde{\Psi}^{(i)}\rangle$'s **differ** (they are only **dihedrally covariant**),
and satisfy **different** linear equations (with $RX_i(t)$)...

...and $\text{Sym } |\tilde{\Psi}^{(i)}\rangle$ does **not** satisfy any simple
linear equation that fixes it univocally!

Best possible hope:

- Find a **new way** $\pi'(\phi)$ of associating link patterns to FPL;
- Find&prove $|\tilde{\Psi}(t)\rangle = |\Psi'(t)\rangle$ **with no need of symmetrization**;
 - Prove **combinatorially** that $\text{Sym } |\Psi'(t)\rangle = \text{Sym } |\Psi(t)\rangle$

Bonus: The new enumeration is interesting by itself

A quest for a new strategy

The strategy in the 2010 RS proof, by L. Cantini and me, was

- Realize that $H|\tilde{\Psi}\rangle = 0$ fixes $|\tilde{\Psi}\rangle$ univocally;
- Prove combinatorially that also $|\Psi\rangle$ satisfies $H|\Psi\rangle = 0$...

...But the $|\tilde{\Psi}^{(i)}\rangle$'s **differ** (they are only **dihedrally covariant**),
and satisfy **different** linear equations (with $RX_i(t)$)...

...and $\text{Sym } |\tilde{\Psi}^{(i)}\rangle$ does **not** satisfy any simple
linear equation that fixes it univocally!

Best possible hope:

- Find a **new way** $\pi'(\phi)$ of associating link patterns to FPL;
- Find&prove $|\tilde{\Psi}(t)\rangle = |\Psi'(t)\rangle$ **with no need of symmetrization**;
 - Prove **combinatorially** that $\text{Sym } |\Psi'(t)\rangle = \text{Sym } |\Psi(t)\rangle$

Bonus: The new enumeration is interesting by itself

A quest for a new strategy

The strategy in the 2010 RS proof, by L. Cantini and me, was

- Realize that $H|\tilde{\Psi}\rangle = 0$ fixes $|\tilde{\Psi}\rangle$ univocally;
- Prove combinatorially that also $|\Psi\rangle$ satisfies $H|\Psi\rangle = 0$...

...But the $|\tilde{\Psi}^{(i)}\rangle$'s **differ** (they are only **dihedrally covariant**),
and satisfy **different** linear equations (with $RX_i(t)$)...

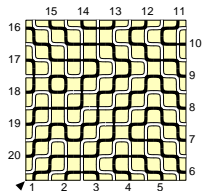
...and $\text{Sym } |\tilde{\Psi}^{(i)}\rangle$ does **not** satisfy any simple
linear equation that fixes it univocally!

Best possible hope:

- Find a **new way** $\pi'(\phi)$ of associating link patterns to FPL;
- Find&prove $|\tilde{\Psi}(t)\rangle = |\Psi'(t)\rangle$ **with no need of symmetrization**;
 - Prove **combinatorially** that $\text{Sym } |\Psi'(t)\rangle = \text{Sym } |\Psi(t)\rangle$

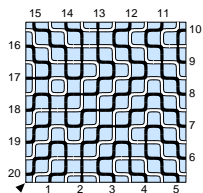
Bonus: The new enumeration is interesting by itself

The heretical enumeration



The role of black and white is symmetrical...

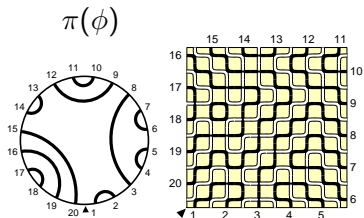
The heretical enumeration



...who's who is a matter of convention.

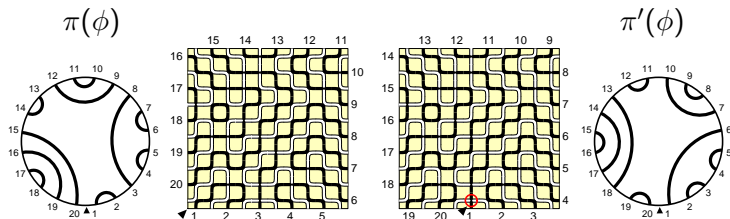
Swapping coloration in **all** FPL's leads to an equivalent conjecture

The heretical enumeration



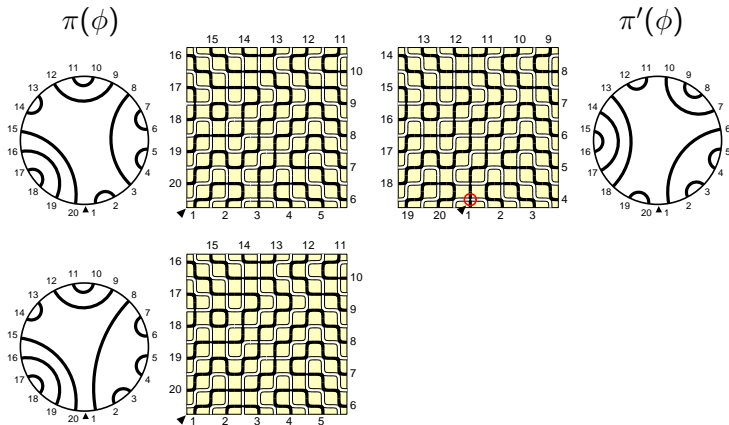
Here's the rule: if the refinement position is **odd**...

The heretical enumeration



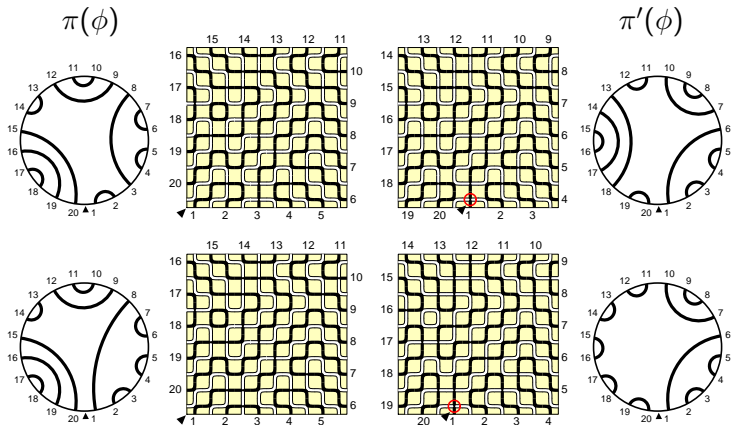
Here's the rule: if the refinement position is **odd**...
...you just **rotate** the starting point to the refinement position

The heretical enumeration



if the refinement position is **even**...

The heretical enumeration



if the refinement position is **even**...

...you **swap** black and white, and **rotate** the starting point

Divide and conquer

We wanted to prove Di Francesco 2004 conjecture:

$$\text{Sym } |\tilde{\Psi}(t)\rangle = \text{Sym } |\Psi(t)\rangle$$

with $|\tilde{\Psi}(t)\rangle$ solving $(X_1(t) - R^{-1})|\tilde{\Psi}(t)\rangle = 0$

$$\text{and } |\Psi(t)\rangle = \sum_{\phi} t^{h(\phi)-1} |\pi(\phi)\rangle$$

We have been led to split this in two parts:

$$|\tilde{\Psi}(t)\rangle = |\Psi'(t)\rangle \quad \text{and} \quad \text{Sym } |\Psi'(t)\rangle = \text{Sym } |\Psi(t)\rangle$$

$$\text{with } |\Psi'(t)\rangle = \sum_{\phi} t^{h(\phi)-1} |\pi'(\phi)\rangle$$

The first relation is proven if you show that
 $(X_1(t) - R^{-1})|\Psi'(t)\rangle \equiv (t\mathbf{1} - R^{-1} - (t-1)e_1)|\Psi'(t)\rangle = 0$

recalling that $e_1^2 = e_1$, and $(1 - e_1)^2 = (1 - e_1)$:

Divide and conquer

We wanted to prove Di Francesco 2004 conjecture:

$$\text{Sym } |\tilde{\Psi}(t)\rangle = \text{Sym } |\Psi(t)\rangle$$

with $|\tilde{\Psi}(t)\rangle$ solving $(X_1(t) - R^{-1})|\tilde{\Psi}(t)\rangle = 0$

$$\text{and } |\Psi(t)\rangle = \sum_{\phi} t^{h(\phi)-1} |\pi(\phi)\rangle$$

We have been led to split this in two parts:

$$|\tilde{\Psi}(t)\rangle = |\Psi'(t)\rangle \quad \text{and} \quad \text{Sym } |\Psi'(t)\rangle = \text{Sym } |\Psi(t)\rangle$$

$$\text{with } |\Psi'(t)\rangle = \sum_{\phi} t^{h(\phi)-1} |\pi'(\phi)\rangle$$

The first relation is proven if you show that
 $(X_1(t) - R^{-1})|\Psi'(t)\rangle \equiv (t\mathbf{1} - R^{-1} - (t-1)e_1)|\Psi'(t)\rangle = 0$

recalling that $e_1^2 = e_1$, and $(1 - e_1)^2 = (1 - e_1)$:

Divide and conquer

We wanted to prove Di Francesco 2004 conjecture:

$$\text{Sym } |\tilde{\Psi}(t)\rangle = \text{Sym } |\Psi(t)\rangle$$

with $|\tilde{\Psi}(t)\rangle$ solving $(X_1(t) - R^{-1})|\tilde{\Psi}(t)\rangle = 0$

$$\text{and } |\Psi(t)\rangle = \sum_{\phi} t^{h(\phi)-1} |\pi(\phi)\rangle$$

We have been led to split this in two parts:

$$|\tilde{\Psi}(t)\rangle = |\Psi'(t)\rangle \quad \text{and} \quad \text{Sym } |\Psi'(t)\rangle = \text{Sym } |\Psi(t)\rangle$$

$$\text{with } |\Psi'(t)\rangle = \sum_{\phi} t^{h(\phi)-1} |\pi'(\phi)\rangle$$

The first relation is proven if you show that
 $(X_1(t) - R^{-1})|\Psi'(t)\rangle \equiv (t\mathbf{1} - R^{-1} - (t-1)e_1)|\Psi'(t)\rangle = 0$

recalling that $e_1^2 = e_1$, and $(1 - e_1)^2 = (1 - e_1)$:

We wanted to prove Di Francesco 2004 conjecture:

$$\text{Sym } |\tilde{\Psi}(t)\rangle = \text{Sym } |\Psi(t)\rangle$$

with $|\tilde{\Psi}(t)\rangle$ solving $(X_1(t) - R^{-1})|\tilde{\Psi}(t)\rangle = 0$

$$\text{and } |\Psi(t)\rangle = \sum_{\phi} t^{h(\phi)-1} |\pi(\phi)\rangle$$

We have been led to split this in two parts:

$$|\tilde{\Psi}(t)\rangle = |\Psi'(t)\rangle \quad \text{and} \quad \text{Sym } |\Psi'(t)\rangle = \text{Sym } |\Psi(t)\rangle$$

$$\text{with } |\Psi'(t)\rangle = \sum_{\phi} t^{h(\phi)-1} |\pi'(\phi)\rangle$$

The first relation is proven if you show that
 $(X_1(t) - R^{-1})|\Psi'(t)\rangle \equiv (t\mathbf{1} - R^{-1} - (t-1)e_1)|\Psi'(t)\rangle = 0$

recalling that $e_1^2 = e_1$, and $(1 - e_1)^2 = (1 - e_1)$:

$$e_1 (t\mathbf{1} - R^{-1} - (t-1)e_1)|\Psi'(t)\rangle = 0$$

$$(1 - e_1) (t\mathbf{1} - R^{-1} - (t-1)e_1)|\Psi'(t)\rangle = 0$$

Divide and conquer

We wanted to prove Di Francesco 2004 conjecture:

$$\text{Sym } |\tilde{\Psi}(t)\rangle = \text{Sym } |\Psi(t)\rangle$$

with $|\tilde{\Psi}(t)\rangle$ solving $(X_1(t) - R^{-1})|\tilde{\Psi}(t)\rangle = 0$

$$\text{and } |\Psi(t)\rangle = \sum_{\phi} t^{h(\phi)-1} |\pi(\phi)\rangle$$

We have been led to split this in two parts:

$$|\tilde{\Psi}(t)\rangle = |\Psi'(t)\rangle \quad \text{and} \quad \text{Sym } |\Psi'(t)\rangle = \text{Sym } |\Psi(t)\rangle$$

$$\text{with } |\Psi'(t)\rangle = \sum_{\phi} t^{h(\phi)-1} |\pi'(\phi)\rangle$$

The first relation is proven if you show that
 $(X_1(t) - R^{-1})|\Psi'(t)\rangle \equiv (t\mathbf{1} - R^{-1} - (t-1)e_1)|\Psi'(t)\rangle = 0$

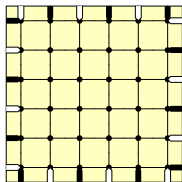
recalling that $e_1^2 = e_1$, and $(1 - e_1)^2 = (1 - e_1)$:

$$e_1 (\mathbf{1} - R^{-1})|\Psi'(t)\rangle = 0$$

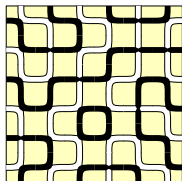
$$(1 - e_1) (t\mathbf{1} - R^{-1})|\Psi'(t)\rangle = 0$$

FPL in fancy domains...

We considered so far FPL in the $n \times n$ square domain, with alternating boundary conditions, i.e. consistent fillings of this:



into things like this:



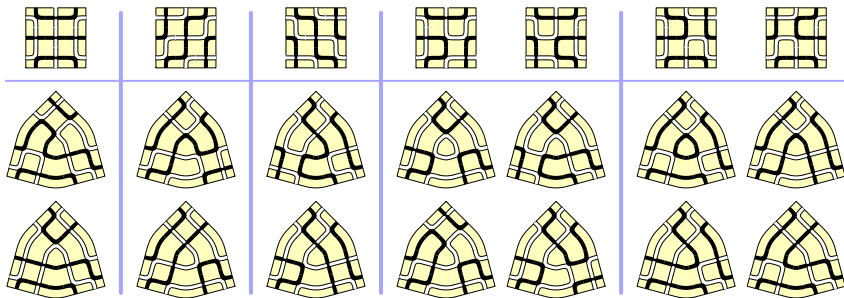
Fully-Packed Loops in different domains

Let's try to compare enumerations in **different** domains,
with the **same** perimeter...



Fully-Packed Loops in different domains

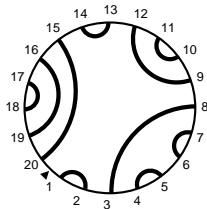
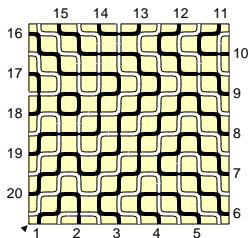
Let's try to compare enumerations in **different** domains,
with the **same** perimeter...



The **Razumov–Stroganov correspondence** holds in this wider family
of domains... is this true also for the **Di Francesco 2004** refinement?

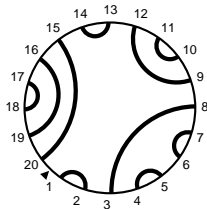
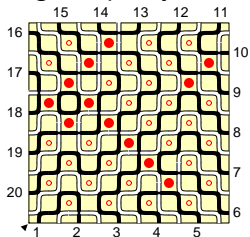
Wieland gyration: how it works

FPL config



Wieland gyration: how it works

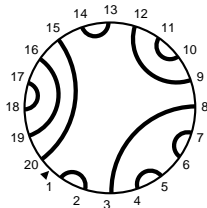
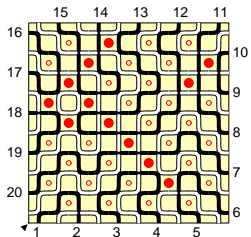
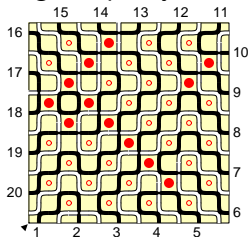
Mark faces  and ,
of given parity



Wieland gyration: how it works

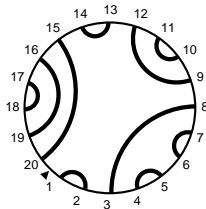
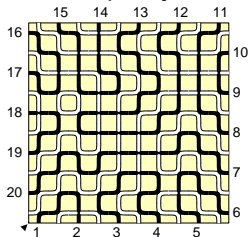
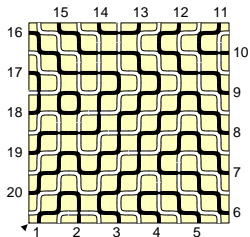
Mark faces  and , Exchange  \leftrightarrow 

of given parity



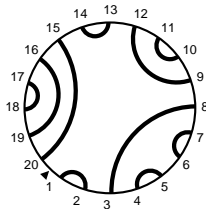
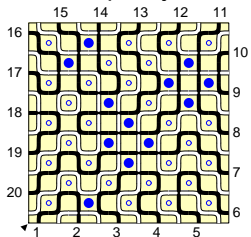
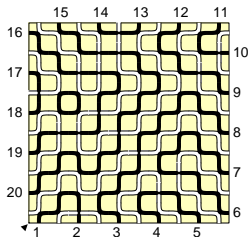
Wieland gyration: how it works

Mark faces  and ,
of other parity



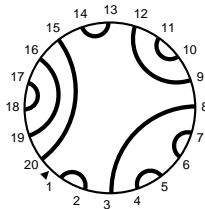
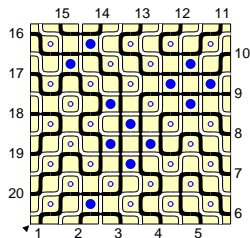
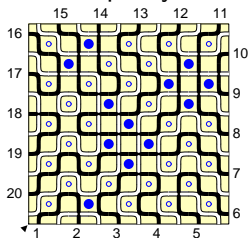
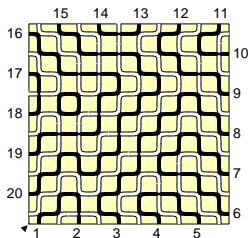
Wieland gyration: how it works

Mark faces  and ,
of other parity

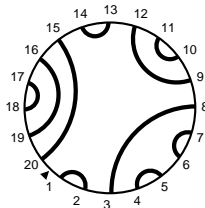
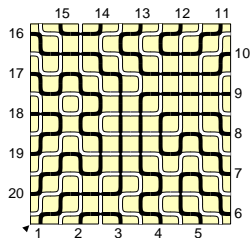
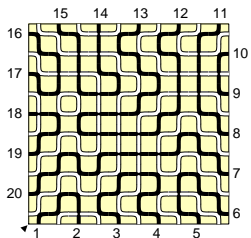
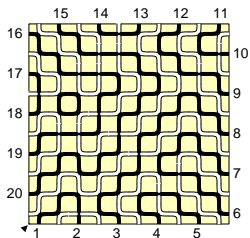


Wieland gyration: how it works

Mark faces  and , Exchange  \leftrightarrow 

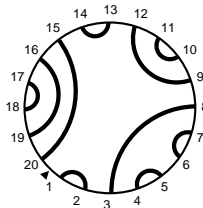
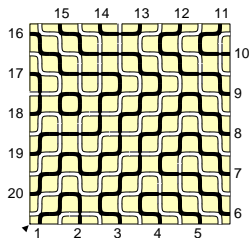


Wieland gyration: how it works

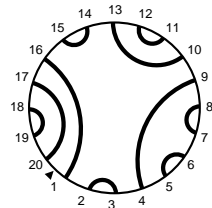
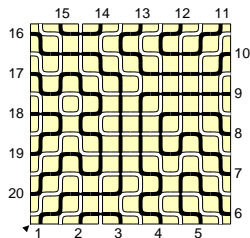
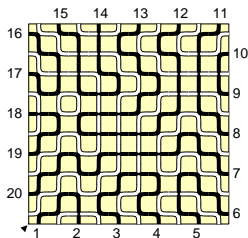


Wieland gyration: how it works

Link pattern $\pi...$



...and $R\pi...$

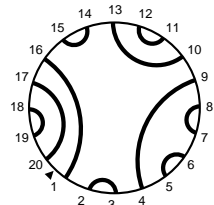
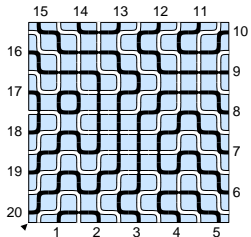
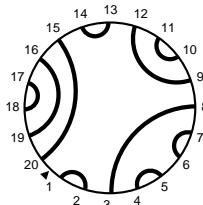
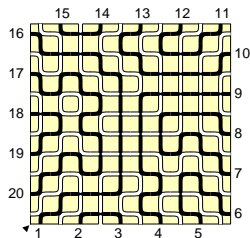
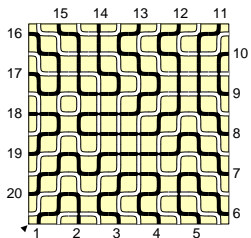
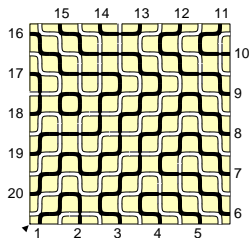


Wieland gyration: how it works

Link pattern $\pi\dots$

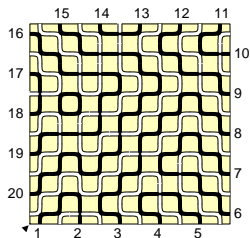
...and, on the conjugate
of the intermediate step...

...and $R\pi\dots$

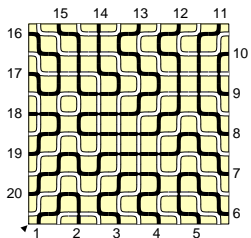


Wieland gyration: how it works

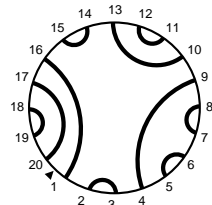
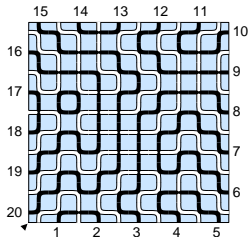
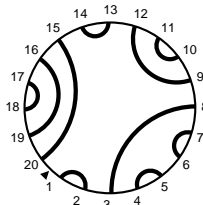
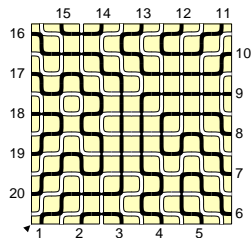
Link pattern $\pi\dots$



$\dots R^{\frac{1}{2}} \pi \dots$

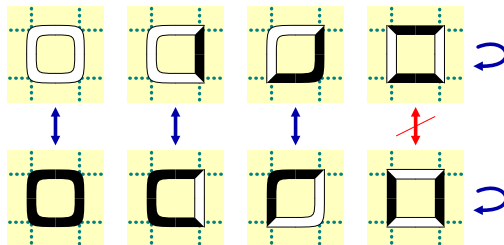


\dots and $R \pi \dots$



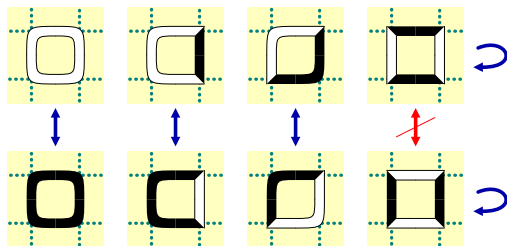
Wieland gyration: why it works

Easier to visualize the $\square \leftrightarrow \square$ exchange on the few \square , \square faces...
...but better use the conjugate config at intermediate step,
and think that \square , \square are **the only faces fixed** in the transformation



Wieland gyration: why it works

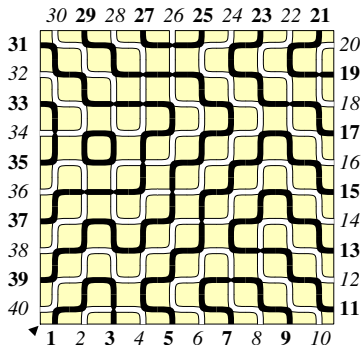
Easier to visualize the $\square \leftrightarrow \square$ exchange on the few \square , \square faces...
...but better use the conjugate config at intermediate step,
and think that \square , \square are **the only faces fixed** in the transformation



This **inverts** $\deg_{\text{black}}(v) \leftrightarrow \deg_{\text{white}}(v)$,
and **preserves** connectivity of open-path endpoints

Wieland gyration: where it works

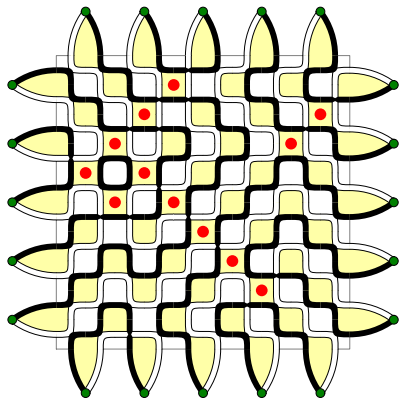
...in the original square domain for FPL we have “external legs” (i.e., vertices of degree 1)... if we **pair** them, to produce triangles, we solve this annoyance...



A configuration on (Λ, τ_+)
(i.e., first leg is black)

Wieland gyration: where it works

...in the original square domain for FPL we have “external legs” (i.e., vertices of degree 1)... if we **pair** them, to produce triangles, we solve this annoyance...

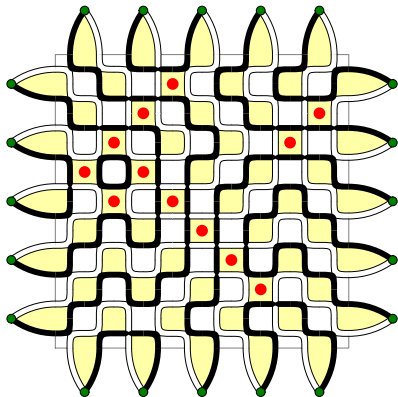


The construction of \mathcal{G}_+ ,
pairing $(2j - 1, 2j)$ legs
(plaquettes are in yellow)

mark in red  and 

Wieland gyration: where it works

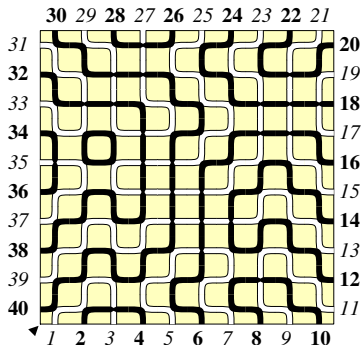
...in the original square domain for FPL we have “external legs” (i.e., vertices of degree 1)... if we **pair** them, to produce triangles, we solve this annoyance...



The result of map H_+

Wieland gyration: where it works

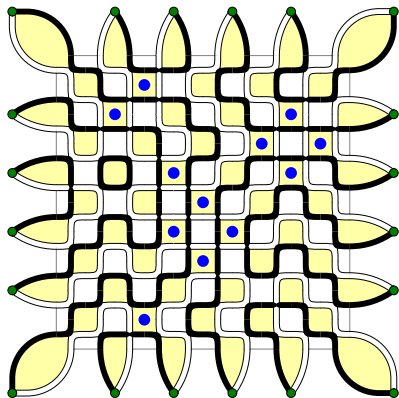
...in the original square domain for FPL we have “external legs” (i.e., vertices of degree 1)... if we **pair** them, to produce triangles, we solve this annoyance...



Split auxiliary vertices
to recover the (Λ, τ_-)
geometry
(i.e., first leg is white)

Wieland gyration: where it works

...in the original square domain for FPL we have “external legs” (i.e., vertices of degree 1)... if we **pair** them, to produce triangles, we solve this annoyance...

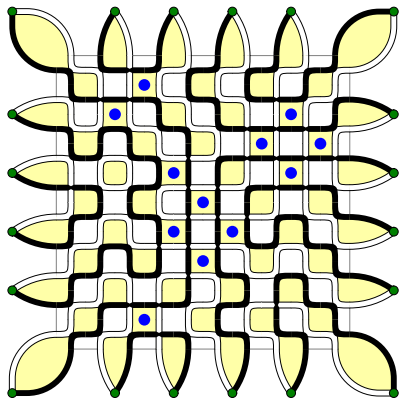


The construction of \mathcal{G}_- ,
pairing $(2j, 2j + 1)$ legs

mark in blue  and 

Wieland gyration: where it works

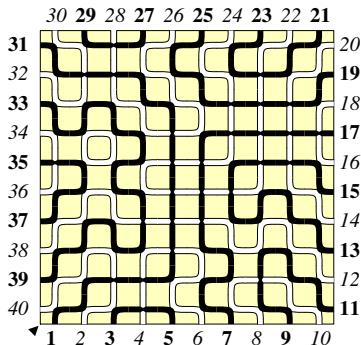
...in the original square domain for FPL we have “external legs” (i.e., vertices of degree 1)... if we **pair** them, to produce triangles, we solve this annoyance...



The result of map H_-

Wieland gyration: where it works

...in the original square domain for FPL we have “external legs” (i.e., vertices of degree 1)... if we **pair** them, to produce triangles, we solve this annoyance...



Split auxiliary vertices to recover the (Λ, τ_+) original geometry (with a rotated link pattern)...

Wieland gyration: where it works

So, the trick is:

- invert $\deg_{\text{black}}(v) \leftrightarrow \deg_{\text{white}}(v)$
- preserve connectivity of open paths

Wieland gyration: where it works

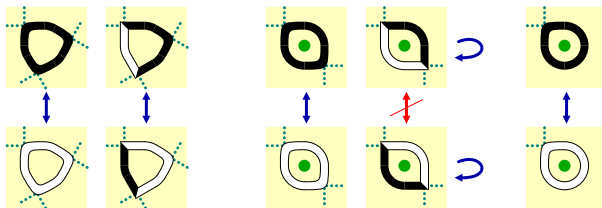
- So, the trick is:
- invert $\deg_{\text{black}}(v) \leftrightarrow \deg_{\text{white}}(v)$
 - preserve connectivity of open paths
- Works with the Wieland recipe, on faces $\ell = 4$

Wieland gyration: where it works

So, the trick is:

- invert $\deg_{\text{black}}(v) \leftrightarrow \deg_{\text{white}}(v)$
- preserve connectivity of open paths

- Works with the Wieland recipe, on faces $\ell = 4$
- Works even more easily on faces $\ell = 1, 2, 3$



Wieland gyration: where it works

So, the trick is:

- invert $\deg_{\text{black}}(v) \leftrightarrow \deg_{\text{white}}(v)$
- preserve connectivity of open paths

- Works with the Wieland recipe, on faces $\ell = 4$
- Works even more easily on faces $\ell = 1, 2, 3$
- **Can't work** at all on faces $\ell \geq 5$

Wieland gyration: where it works

So, the trick is:

- invert $\deg_{\text{black}}(v) \leftrightarrow \deg_{\text{white}}(v)$
- preserve connectivity of open paths

- Works with the Wieland recipe, on faces $\ell = 4$
- Works even more easily on faces $\ell = 1, 2, 3$
- **Can't work** at all on faces $\ell \geq 5$
- At boundaries, pair external legs to produce triangles

Wieland gyration: where it works

So, the trick is:

- invert $\deg_{\text{black}}(v) \leftrightarrow \deg_{\text{white}}(v)$
- preserve connectivity of open paths

- Works with the Wieland recipe, on faces $\ell = 4$
- Works even more easily on faces $\ell = 1, 2, 3$
- **Can't work** at all on faces $\ell \geq 5$
- At boundaries, pair external legs to produce triangles

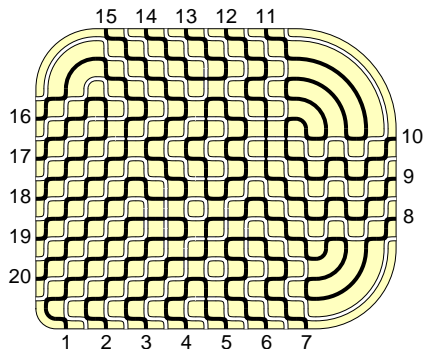
A **single** move exists on plenty of graphs...

then, **rotation** comes from **two** moves

...many more domains than just $n \times n$ squares have this property!

Wieland gyration: where it works

Thus you can trade corners for points of curvature (i.e., faces with less than 4 sides)

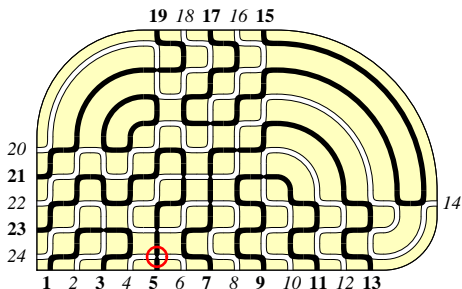


(bottom line: an **elementary** generalization of Wieland strategy gives **rotational symmetry** for FPL enumerations above)

Examples of domains with dihedral invariance...

(...and with refined Razumov–Stroganov correspondence...)

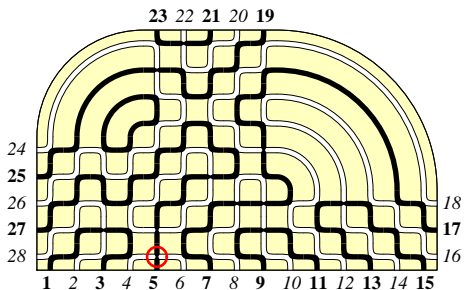
1 corner, 3 triangles:



Examples of domains with dihedral invariance...

(...and with refined Razumov–Stroganov correspondence...)

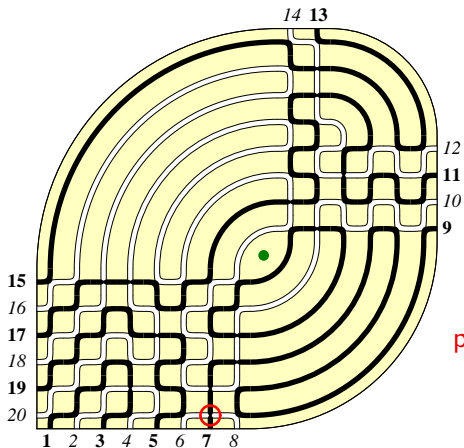
2 corners, 2 triangles:



Examples of domains with dihedral invariance...

(...and with refined Razumov–Stroganov correspondence...)

1 corner, 1 face with $\ell = 2$:

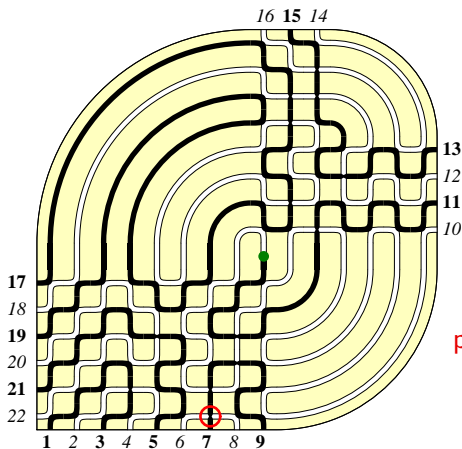


(this works with
punctured link patterns!)

Examples of domains with dihedral invariance...

(...and with refined Razumov–Stroganov correspondence...)

1 corner, 1 degree-2 vertex:

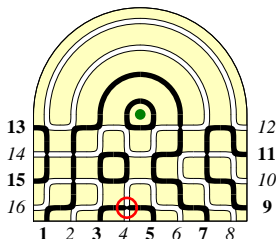
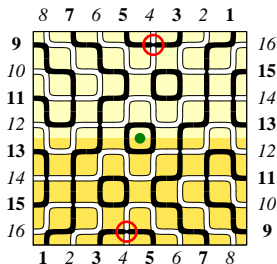


(this works with
punctured link patterns!)

Examples of domains with dihedral invariance...

(...and with refined Razumov–Stroganov correspondence...)

2 corners, 1 face with $\ell = 2$:
(these are HTASM,
half-turn symmetric ASM's)

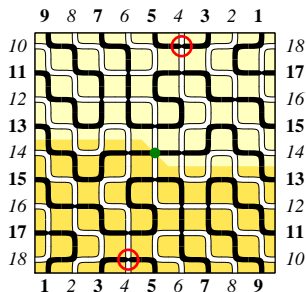


$$L = 2n$$

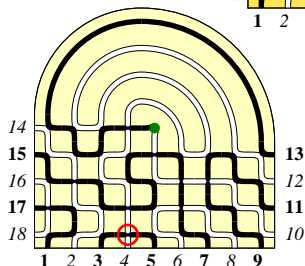
Examples of domains with dihedral invariance...

(...and with refined Razumov–Stroganov correspondence...)

2 corners, 1 face with $\ell = 2$:
(these are HTASM,
half-turn symmetric ASM's)



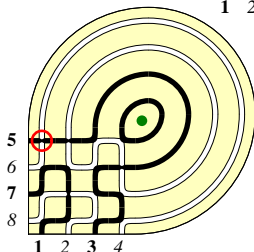
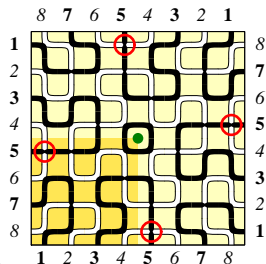
$$L = 2n + 1$$



Examples of domains with dihedral invariance...

(...and with refined Razumov–Stroganov correspondence...)

2 corners, 1 face with $\ell = 2$:
(these are QTASM,
quarter-turn symmetric ASM's)

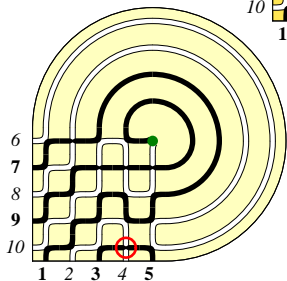
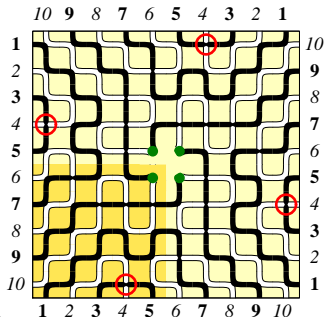


$$L = 4n$$

Examples of domains with dihedral invariance...

(...and with refined Razumov–Stroganov correspondence...)

2 corners, 1 face with $\ell = 2$:
(these are q QTASM,
quasi-quarter-turn symmetric ASM's)



$$L = 4n + 2$$

Yet one word on gyration... the boundary conditions

We have seen how to generalise the **domain**,
using black/white alternating boundary conditions

What does it happen if we generalise on **boundary conditions**?

Pairing consecutive legs with the same colour produces arcs,
and “**loses link-pattern information**”: gyration holds for
linear combinations of $\Psi(\pi)$, instead of component-wise.

These linear combinations, induced by arcs, are well-described by
Temperley-Lieb operators.

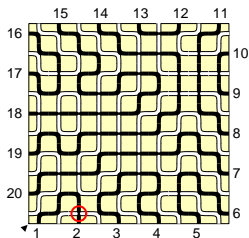
We will not need this in full generality. . .

the study of **a single defect** is sufficient at our purposes.

Alternating boundary conditions, with one defect

Example: the state $|\Psi^{[j]}\rangle = \sum_{\phi: h(\phi)=j} |\pi'(\phi)\rangle$ satisfies

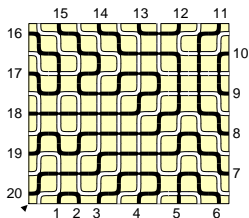
$$(R e_{j-1} - e_j)|\Psi^{[j]}\rangle = 0$$



Alternating boundary conditions, with one defect

Example: the state $|\Psi^{[j]}\rangle = \sum_{\phi: h(\phi)=j} |\pi'(\phi)\rangle$ satisfies

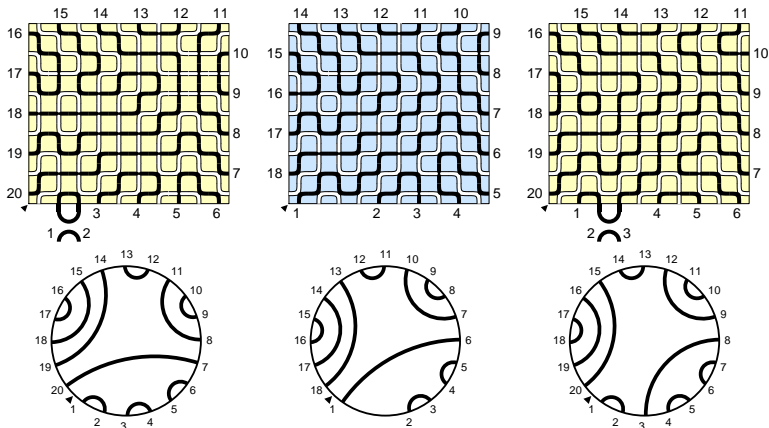
$$(R e_{j-1} - e_j) |\Psi^{[j]}\rangle = 0$$



Alternating boundary conditions, with one defect

Example: the state $|\Psi^{[j]}\rangle = \sum_{\phi: h(\phi)=j} |\pi'(\phi)\rangle$ satisfies

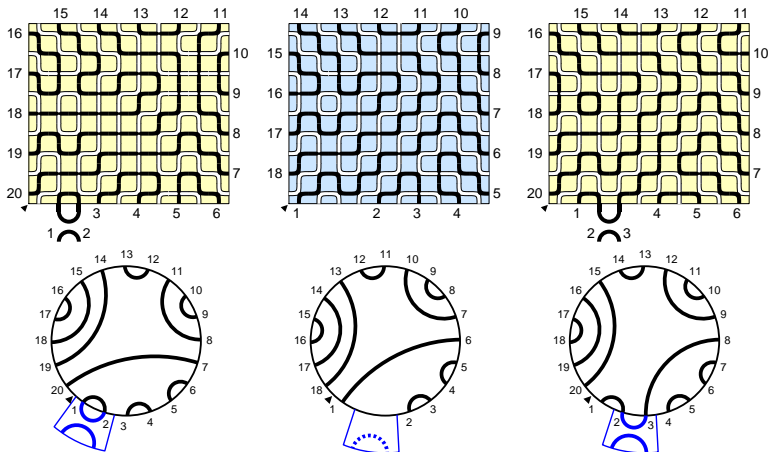
$$(R e_{j-1} - e_j) |\Psi^{[j]}\rangle = 0$$



Alternating boundary conditions, with one defect

Example: the state $|\Psi^{[j]}\rangle = \sum_{\phi: h(\phi)=j} |\pi'(\phi)\rangle$ satisfies

$$(R e_{j-1} - e_j) |\Psi^{[j]}\rangle = 0$$



A first consequence

Recall our checklist of identities:

$$1 : e_1 (\mathbf{1} - R^{-1}) |\Psi'(t)\rangle = 0$$

$$2 : (1 - e_1) (t\mathbf{1} - R^{-1}) |\Psi'(t)\rangle = 0$$

$$3 : \text{Sym} |\Psi'(t)\rangle = \text{Sym} |\Psi(t)\rangle$$

(2) is equivalent to ask that $t\Psi(t; \pi) = \Psi(t; R^{-1}\pi)$,
for all π such that $1 \approx 2 \dots$

but this is easily seen: $1 \approx 2$ forces a small region, that in turns
implies a simple behaviour of the refinement position under
gyration

A first consequence

Recall our checklist of identities:

1 : $e_1 (\mathbf{1} - R^{-1})|\Psi'(t)\rangle = 0$ ✓ We have just proven this!

2 : $(1 - e_1) (t\mathbf{1} - R^{-1})|\Psi'(t)\rangle = 0$

3 : $\text{Sym} |\Psi'(t)\rangle = \text{Sym} |\Psi(t)\rangle$

(2) is equivalent to ask that $t\Psi(t; \pi) = \Psi(t; R^{-1}\pi)$,
for all π such that $1 \approx 2 \dots$

but this is easily seen: $1 \approx 2$ forces a small region, that in turns
implies a simple behaviour of the refinement position under
gyration

A first consequence

Recall our checklist of identities:

1 : $e_1 (\mathbf{1} - R^{-1})|\Psi'(t)\rangle = 0$ ✓ We have just proven this!

2 : $(1 - e_1) (t\mathbf{1} - R^{-1})|\Psi'(t)\rangle = 0$

3 : $\text{Sym} |\Psi'(t)\rangle = \text{Sym} |\Psi(t)\rangle$

(2) is equivalent to ask that $t\Psi(t; \pi) = \Psi(t; R^{-1}\pi)$,
for all π such that $1 \approx 2 \dots$

but this is easily seen: $1 \approx 2$ forces a small region, that in turns implies a simple behaviour of the refinement position under gyration

A first consequence

Recall our checklist of identities:

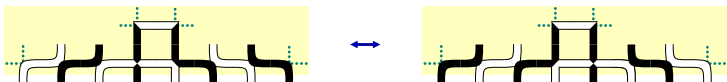
1 : $e_1 (\mathbf{1} - R^{-1})|\Psi'(t)\rangle = 0$ ✓ We have just proven this!

2 : $(1 - e_1) (t\mathbf{1} - R^{-1})|\Psi'(t)\rangle = 0$ ✓ Done!

3 : $\text{Sym} |\Psi'(t)\rangle = \text{Sym} |\Psi(t)\rangle$

(2) is equivalent to ask that $t\Psi(t; \pi) = \Psi(t; R^{-1}\pi)$,
for all π such that $1 \approx 2 \dots$

but this is easily seen: $1 \approx 2$ forces a small region, that in turns
implies a simple behaviour of the refinement position under
gyration



A first consequence

Recall our checklist of identities:

1 : $e_1 (\mathbf{1} - R^{-1})|\Psi'(t)\rangle = 0$ ✓ We have just proven this!

2 : $(1 - e_1) (t\mathbf{1} - R^{-1})|\Psi'(t)\rangle = 0$ ✓ Done!

3 : $\text{Sym} |\Psi'(t)\rangle = \text{Sym} |\Psi(t)\rangle$ ➡ Look at gyration even better!

(2) is equivalent to ask that $t\Psi(t; \pi) = \Psi(t; R^{-1}\pi)$,
for all π such that $1 \approx 2 \dots$

but this is easily seen: $1 \approx 2$ forces a small region, that in turns
implies a simple behaviour of the refinement position under
gyration



A final observation on the orbits

Consider the **orbits** under Wieland half-gyration

As FPL in the same orbit have the same link pattern up to rotation,

$\text{Sym} |\Psi'(t)\rangle = \text{Sym} |\Psi(t)\rangle$ follows if, for every j , and every orbit, there are as many contributions t^{j-1} to $|\Psi'(t)\rangle$ as to $|\Psi(t)\rangle$.

Study the behavior of the **trajectory** $h(x)$ of the refinement position:

- ▶ $h(x+1) - h(x) \in \{0, \pm 1\}$
- ▶ In a periodic function, a height value is attained alternately on ascending and descending portions (if not at maxima/minima)
- ▶ All maxima/minima plateaux have length 2, the rest has slope ± 1
- ▶ Ascending/descending parts of the trajectory have respectively black and white refinement position

A final observation on the orbits

Consider the **orbits** under Wieland half-gyration

As FPL in the same orbit have the same link pattern up to rotation, $\text{Sym} |\Psi'(t)\rangle = \text{Sym} |\Psi(t)\rangle$ follows if, for every j , and every orbit, there are as many contributions t^{j-1} to $|\Psi'(t)\rangle$ as to $|\Psi(t)\rangle$.

Study the behavior of the **trajectory** $h(x)$ of the refinement position:

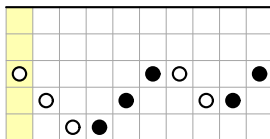
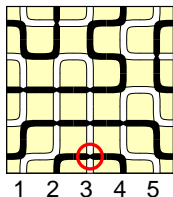
- ▶ $h(x+1) - h(x) \in \{0, \pm 1\}$
- ▶ In a periodic function, a height value is attained alternately on ascending and descending portions (if not at maxima/minima)
- ▶ All maxima/minima plateaux have length 2, the rest has slope ± 1
- ▶ Ascending/descending parts of the trajectory have respectively black and white refinement position

A final observation on the orbits

As a consequence, in any orbit O , and for any value j , the numbers of $\phi \in O$ such that $h(\phi) = j$, and

- ▶ are in even (resp. odd) position in the orbit;
- ▶ or have a black (resp. white) refinement position;

are all equal. This completes the proof.

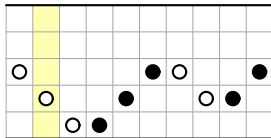
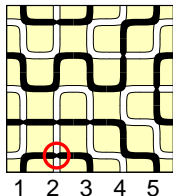


A final observation on the orbits

As a consequence, in any orbit O , and for any value j , the numbers of $\phi \in O$ such that $h(\phi) = j$, and

- ▶ are in even (resp. odd) position in the orbit;
- ▶ or have a black (resp. white) refinement position;

are all equal. This completes the proof.

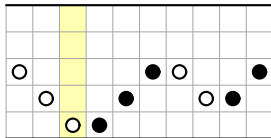
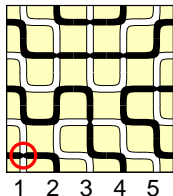


A final observation on the orbits

As a consequence, in any orbit O , and for any value j , the numbers of $\phi \in O$ such that $h(\phi) = j$, and

- ▶ are in even (resp. odd) position in the orbit;
- ▶ or have a black (resp. white) refinement position;

are all equal. This completes the proof.

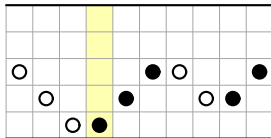
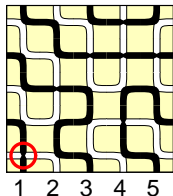


A final observation on the orbits

As a consequence, in any orbit O , and for any value j , the numbers of $\phi \in O$ such that $h(\phi) = j$, and

- ▶ are in even (resp. odd) position in the orbit;
- ▶ or have a black (resp. white) refinement position;

are all equal. This completes the proof.

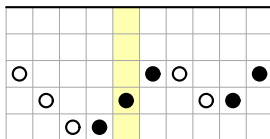
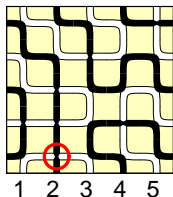


A final observation on the orbits

As a consequence, in any orbit O , and for any value j , the numbers of $\phi \in O$ such that $h(\phi) = j$, and

- ▶ are in even (resp. odd) position in the orbit;
- ▶ or have a black (resp. white) refinement position;

are all equal. This completes the proof.

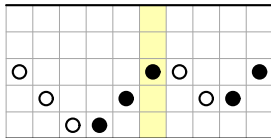
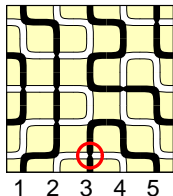


A final observation on the orbits

As a consequence, in any orbit O , and for any value j , the numbers of $\phi \in O$ such that $h(\phi) = j$, and

- ▶ are in even (resp. odd) position in the orbit;
- ▶ or have a black (resp. white) refinement position;

are all equal. This completes the proof.

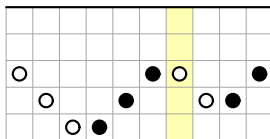
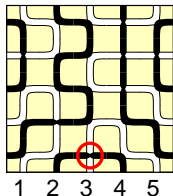


A final observation on the orbits

As a consequence, in any orbit O , and for any value j , the numbers of $\phi \in O$ such that $h(\phi) = j$, and

- ▶ are in even (resp. odd) position in the orbit;
- ▶ or have a black (resp. white) refinement position;

are all equal. This completes the proof.

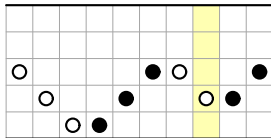
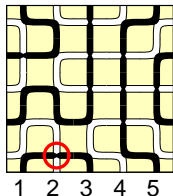


A final observation on the orbits

As a consequence, in any orbit O , and for any value j , the numbers of $\phi \in O$ such that $h(\phi) = j$, and

- ▶ are in even (resp. odd) position in the orbit;
- ▶ or have a black (resp. white) refinement position;

are all equal. This completes the proof.

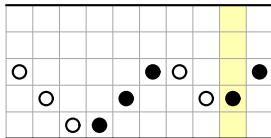
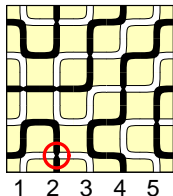


A final observation on the orbits

As a consequence, in any orbit O , and for any value j , the numbers of $\phi \in O$ such that $h(\phi) = j$, and

- ▶ are in even (resp. odd) position in the orbit;
- ▶ or have a black (resp. white) refinement position;

are all equal. This completes the proof.

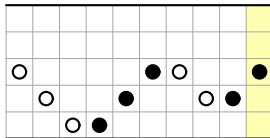
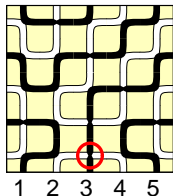


A final observation on the orbits

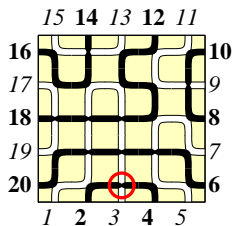
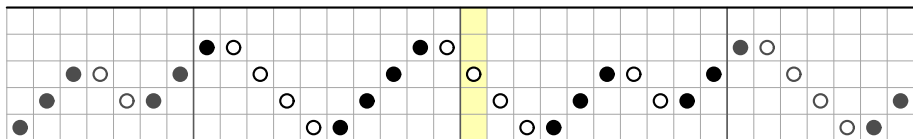
As a consequence, in any orbit O , and for any value j , the numbers of $\phi \in O$ such that $h(\phi) = j$, and

- ▶ are in even (resp. odd) position in the orbit;
- ▶ or have a black (resp. white) refinement position;

are all equal. This completes the proof.

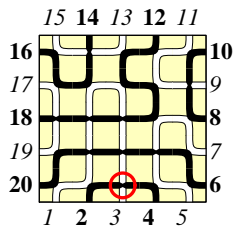
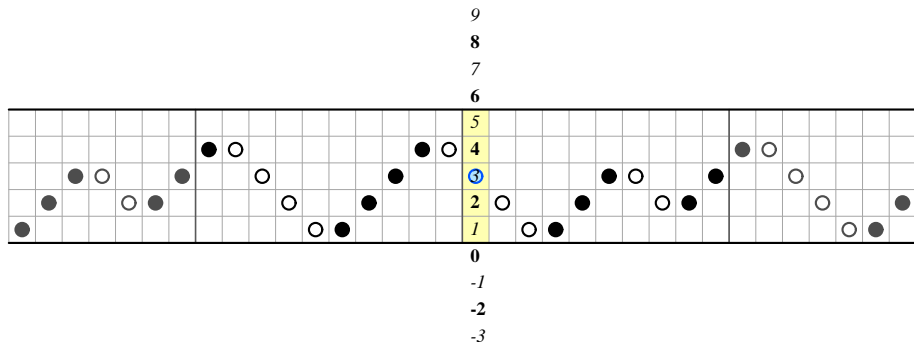


A bijective version of the last lemma



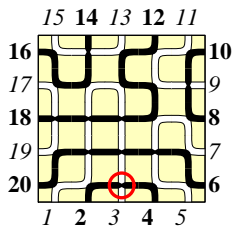
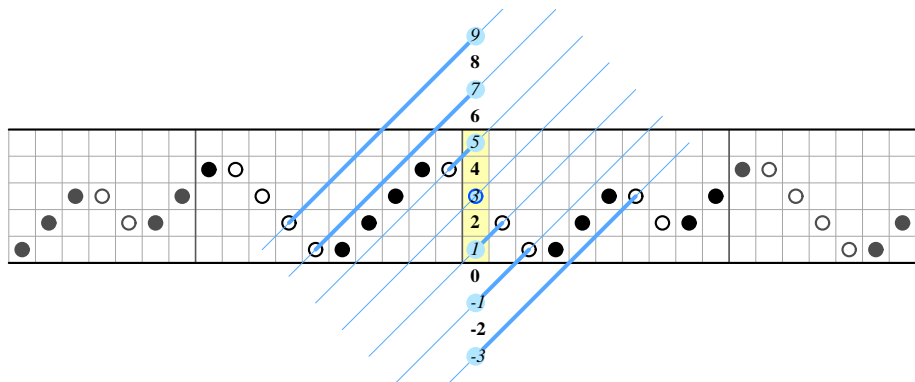
The structure of the orbits gives
a **bijection factory**...

A bijective version of the last lemma



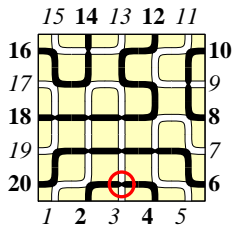
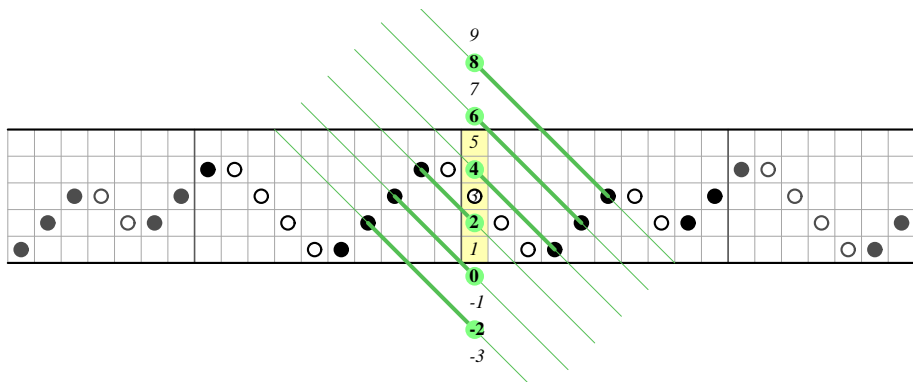
Consider the infinite orbit, and extend ordinates from $\{1, \dots, L\}$ to $\mathbb{Z} \dots$

A bijective version of the last lemma



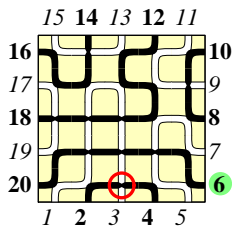
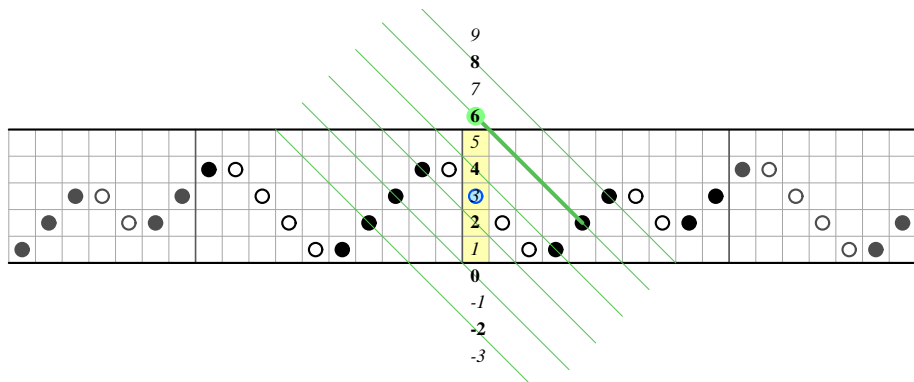
All 45-degree diagonals with odd intercept have a **unique** white intersection

A bijective version of the last lemma



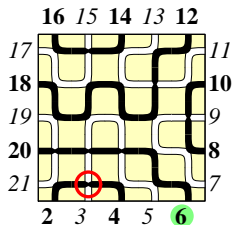
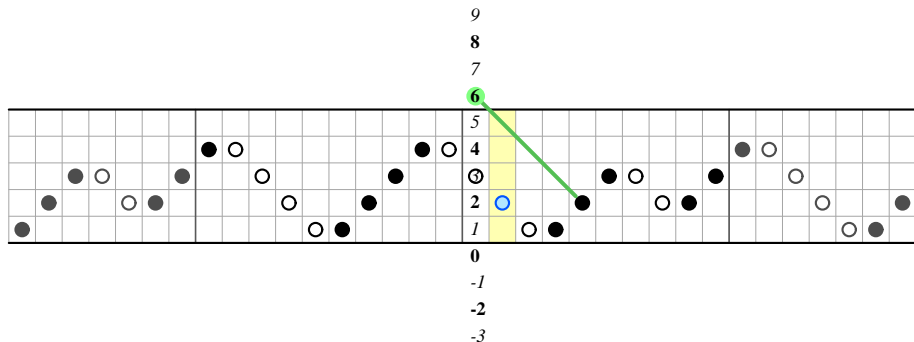
All 135-degree diagonals with even intercept have a **unique** black intersection

A bijective version of the last lemma



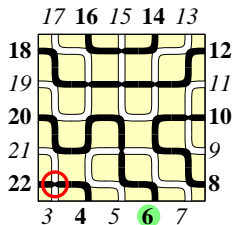
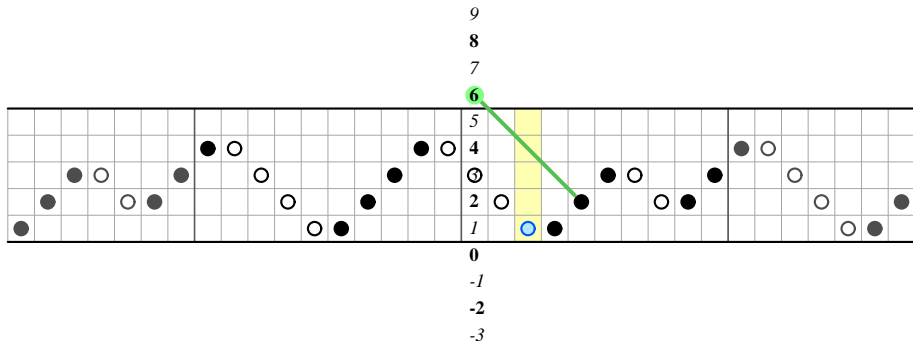
This implies that, for any integer c , there is a **unique** config in the orbit with refinement position on leg c !

A bijective version of the last lemma



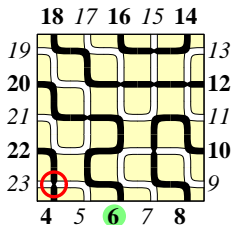
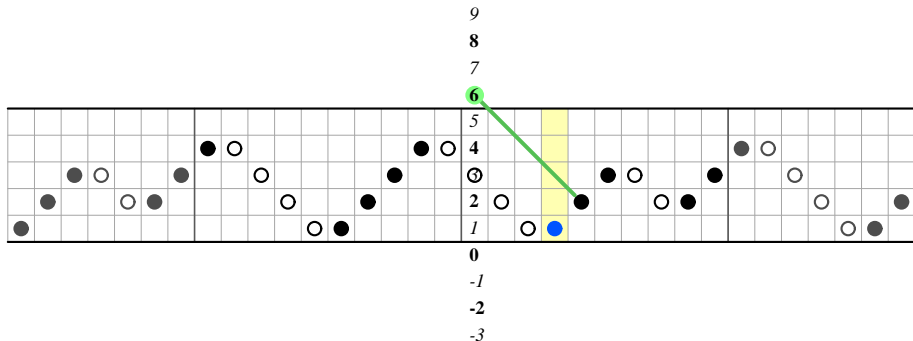
This implies that, for any integer c , there is a **unique** config in the orbit with refinement position on leg c !

A bijective version of the last lemma



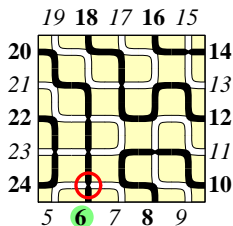
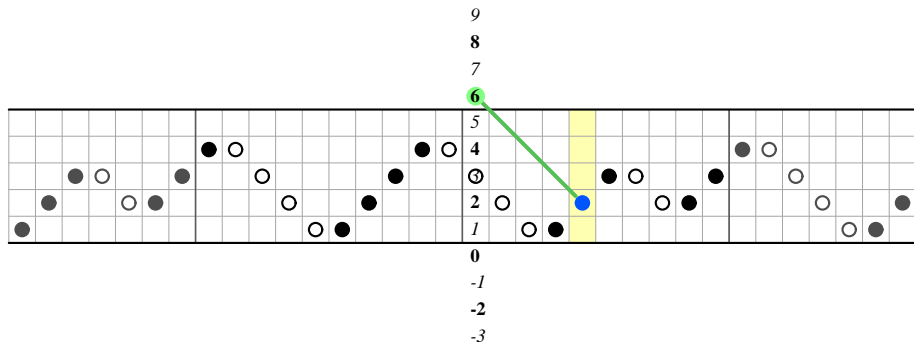
This implies that, for any integer c , there is a **unique** config in the orbit with refinement position on leg c !

A bijective version of the last lemma



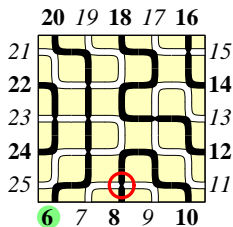
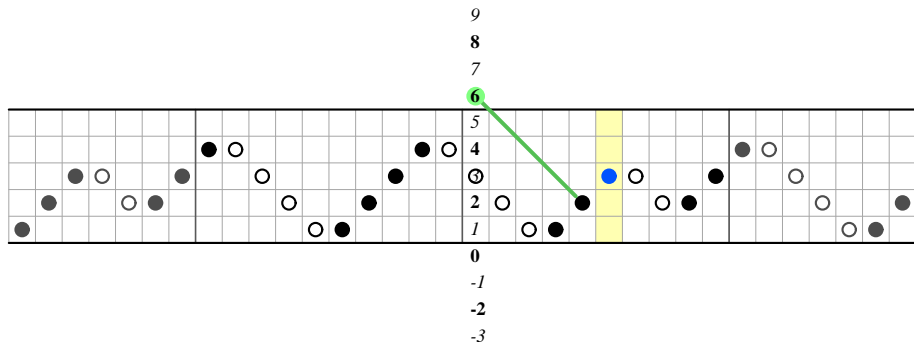
This implies that, for any integer c , there is a **unique** config in the orbit with refinement position on leg c !

A bijective version of the last lemma



This implies that, for any integer c , there is a **unique** config in the orbit with refinement position on leg c !

A bijective version of the last lemma



This implies that, for any integer c , there is a **unique** config in the orbit with refinement position on leg c !

A possible conclusion...

In 2010 we had a proof of the **Razumov–Stroganov correspondence**

At first, we wanted to generalize this proof to the **refined** version by Di Francesco, with **one spectral parameter** “turned on”

At last, we did it, by introducing a **new** “heretical” way of associating link patterns to FPL

This leads to a **stronger** statement, and to a new **perspective** on this family of correspondences

Will this help in the determination of correspondences with **more spectral parameters** “turned on”?

Some bibliography

D.P. Robbins,

The story of 1, 2, 7, 42, 429, 7436,...

Math. Intelligencer, 1991

D.M. Bressoud and J. Propp,

How the Alternating Sign Matrix Conjecture was solved Not. AMS, 1999

Lecture Notes of Les Houches Summer School, session 89, July 2008

Exact Methods in Low-dim. Statistical Physics and Quantum Computing

6 B. Nienhuis *Loop models*

7 N. Reshetikhin *Integrability of the 6-vertex model*

17 P. Zinn-Justin *Integrability and combinatorics: selected topics*

L. Cantini, A. Sportiello, *Proof of the Razumov–Stroganov conjecture*,
arXiv:1003.3376, J. Comb. Theory series A **118** (2011) 1549-1574

A one-parameter refinement of the Razumov–Stroganov correspondence,
to appear

(End of the talk)